HAL
open science

The mafic-silicic layered intrusions of Saint-Jean-du-Doigt (France) and North-Guernsey (Channel Islands), Armorican Massif: Gabbro-diorite layering and mafic cumulate-pegmatoid association

Martial Caroff, Nolwenn Coint, Erwan Hallot, Cédric Hamelin, Jean-Jacque Peucat, Gilles Charreteur

To cite this version:

Martial Caroff, Nolwenn Coint, Erwan Hallot, Cédric Hamelin, Jean-Jacque Peucat, et al.. The mafic-silicic layered intrusions of Saint-Jean-du-Doigt (France) and North-Guernsey (Channel Islands), Armorican Massif: Gabbro-diorite layering and mafic cumulate-pegmatoid association. Lithos, 2011, 125, pp.675-692. 10.1016/j.lithos.2011.03.019 . insu-00589245

HAL Id: insu-00589245

https://insu.hal.science/insu-00589245v1

Submitted on 28 Apr 2011

HAL is a multi-disciplinary open access archive for the deposit and dissemination of scientific research documents, whether they are published or not. The documents may come from teaching and research institutions in France or abroad, or from public or private research centers.

L'archive ouverte pluridisciplinaire **HAL**, est destinée au dépôt et à la diffusion de documents scientifiques de niveau recherche, publiés ou non, émanant des établissements d'enseignement et de recherche français ou étrangers, des laboratoires publics ou privés.

The mafic-silicic layered intrusions of Saint-Jean-du-Doigt (France) and North-Guernsey (Channel Islands), Armorican Massif: gabbro-diorite layering and mafic cumulate-pegmatoid association

Martial Caroff [a,*], Nolwenn Coint [a,1], Erwan Hallot [b], Cédric Hamelin [a,2], Jean-Jacques Peucat [b], Gilles Charreteur [b]

[a] UMR CNRS 6538 « Domaines Océaniques », IUEM, Université de Brest, 6 avenue Victor Le Gorgeu, CS 93837, 29238 Brest cedex 3, France

[b] Géosciences Rennes, UMR CNRS 6118, Université de Rennes 1, 35042 Rennes cedex, France

* Corresponding author: caroff@univ-brest.fr

[1] Present address : Department of Geosciences, Texas Tech University, Lubbock, TX 79409, USA (nolwenn.coint@ttu.edu)

[2] Present address : IPGP, Laboratoire de Géosciences Marines, 4, Place Jussieu 75252 Paris cedex 05, France

Abstract

The Saint-Jean-du-Doigt (France) and North-Guernsey (Channel Islands) Intrusive Complexes (hereafter referred to as SJIC and NGIC, respectively) are examples of mafic-silicic layered intrusions in the Armorican Massif. Both are characterized by the occurrence of (1) a basal/peripheral gabbroic unit interlayered with sheets (generally dioritic in composition, occasionally gabbroic) and crossed by leucocratic diapirs and pipes (from monzodioritic to Q-monzonitic in composition), (2) peripheral pegmatoids associated with mafic cumulates and (3) coeval granitoids. Beside these main similarities, some contrasted features lead us to propose two distinct models of formation. The Variscan SJIC includes tholeiitic mafic rocks (monzogabbro) that locally mingle and mix with leucocratic components (monzonite or Q-monzonite). The Cadomian NGIC is calc-alkaline. The SJIC sheet-bearing gabbro is homogeneous from a petrologic point of view, whereas the NGIC exhibits gabbroic macrorhythmic sequences with mineral layering. The Sr-Nd isotopic compositions of the SJIC gabbros are significantly different from those of the associated dioritic layers. This is not the case in the NGIC where the magmas could be cogenetic. We argue that the SJIC gabbro was a liquid that crystallized *in situ* without significant crystal settling. By contrast, the rhythmic sequences of the NGIC are consistent with crystal accumulation. Subsequently, both can be seen as mafic reservoirs which were repeatedly invaded by magmas of intermediate composition. We interpret the sheets in the SJIC as the result of horizontal spreading of dioritic metastable magmas into a gabbroic reservoir crystallizing from below, at levels of neutral buoyancy. Injections and convection in the central part of the reservoir possibly resulted in spectacular mixing/mingling structures. In the NGIC, the emplacement of the dioritic sheets was rather controlled by pre-existing rhythmic cumulative structures. In both intrusions, late differentiated diapirs were extracted from the dioritic sheets. Associated

peripheral pegmatoids are thought to result from the crystallization of liquids issued from a mafic intercumulus melt in the presence of a fluid phase. This extraction might have been enhanced by the disruption of the peripheral cumulate stack, perhaps following pressure drops.

Keywords: Gabbro; Diorite; Granite; Layered intrusion; Replenishment; Armorican Massif

1. Introduction

The term MASLI (MAfic-Silicic Layered Intrusion), as first proposed by Wiebe (1993a and b), refers to plutonic complexes with interlayered mafic (gabbroic) and intermediate/felsic (dioritic to granitic) rocks (Wiebe, 1996; Franceschelli et al., 2005). MASLIs can be recognized by distinctive field relationships which always include (i) lobate contacts between the main gabbro-dioritic intrusions and surrounding or underlying granitic/granodioritic plutons and (ii) layers, sheets, diapirs, and/or veins of dioritic/silicic material into gabbroic units (Wiebe, 1996). Other features commonly (but not always) described in such complexes are: (iii) macrorhythmic gabbro-dioritic units, from less than one to several tens of meters thick, with chilled bases (Wiebe, 1993b, 1994, 1996; Waight et al., 2007), (iv) modal layering and feldspar lamination in the dioritic/silicic layers (Wiebe, 1996), (v) mafic/intermediate enclaves in the granites (Wiebe, 1994; Wiebe et al., 1997), and (vi) basaltic pillow-like chilled bodies within felsic units (Wiebe, 1974, 1993b; Wiebe et al., 2001). Although differences exist between the examples, Wiebe and others first proposed a comprehensive model to account for these features: repeated mafic injections into a felsic chamber, from dioritic to granitic composition, followed by fractional crystallization and complex liquid-liquid (and/or partially crystallized magma-magma) interactions including

70 small scale diapirism and hybridization. More recently, MASLIs were recognized to result
71 from multiple replenishments of mafic and felsic magmas, mingling and limited mixing, and
72 rejuvenation of granite (Wiebe et al., 2007).

73 If the Cadomian layered gabbro-diorite complex of North-Guernsey (Channel Islands)
74 was suspected by Wiebe (1996) to be a MASLI, the Variscan intrusion of Saint-Jean-du-Doigt
75 (France) was never considered as such. However, both Armorican plutonic bodies display
76 many of the features characteristic of mafic-silicic layered intrusions. Additionally, both
77 complexes show spectacular pegmatoid (gabbroic pegmatite) occurrences systematically
78 associated with coarse-grained mafic cumulates. Such a lithologic association has already
79 been described in various gabbroic intrusions (Smartville intrusive complex, California:
80 Beard and Day, 1986; Kraemer macrodyke, Greenland: Momme and Wilson, 2002; Mount
81 Sheridan gabbro, Oklahoma: McEllen, 2006), but not specifically in MASLIs. In spite of their
82 similarities, each Armorican intrusion shows distinctive petrological and geochemical
83 (isotopic) characters.

84 The aim of this study is to reexamine the published models of MASLI formation
85 through these two new examples from the Armorican Massif, which display both shared and
86 contrasted features. This leads us to propose distinct processes of construction emphasizing
87 the possibility that replenishment of mafic chambers by intermediate partially crystallized
88 magmas explains some features of MASLIs.

89

90 **2. Analytical techniques**

91

92 Compositions of mineral phases were obtained with a Cameca SX50 automated
93 electron microprobe (Microsonde Ouest, Brest). Analytical conditions were 15 kV, 15 nA,

counting time 6 s, correction by the ZAF method. Concentrations <0.3% are considered qualitative.

Major and trace element compositions (Table 1) were measured at the University of Brest on whole rock powders by inductively coupled plasma atomic emission spectrometry (ICP-AES). Analytical methods are described in Cotten et al. (1995). Relative standard deviations are <2% for major elements and <5% for trace elements. For the coarsest-grained samples, a large quantity of rock was crushed in a steel jaw-crusher (e.g., 20 kg for the pegmatoid SJ16). After the crushed rock was quartered, a representative split was pulverized in an agate mill.

The Sr-Nd isotopic compositions were obtained from whole rock powders with a Cameca TSN 206 mass spectrometer (Guernsey) and with a Finnigan MAT 262 mass spectrometer (Saint-Jean-du Doigt) at Géosciences Rennes. Sr, Rb, Sm and Nd contents were measured by isotope dilution except for the SJIC samples in which Rb was determined by ICP-AES. Errors on $^{87}Rb/^{86}Sr$ and $^{147}Sm/^{144}Nd$ ratios are 2% and 1%, respectively. Details of analytical procedures are described in Peucat et al. (1999). $^{87}Sr/^{86}Sr$ ratios were normalized to the NBS 987 standard ($^{87}Sr/^{86}Sr = 0.71025$) and $^{143}Nd/^{144}Nd$ ratios to the AMES standard ($^{143}Nd/^{144}Nd = 0.511963$). ε_{Nd} values, in Table 2, were calculated using $^{143}Nd/^{144}Nd_{CHUR} = 0.51264$ and $^{147}Sm/^{144}Nd_{CHUR} = 0.1967$. They correspond to: $\varepsilon_{(0)} = 10^4((^{143}Nd/^{144}Nd_{sample}/051264) -1)$ and $\varepsilon_{(t)} = \varepsilon_{(0)} -(25.1((^{147}Sm/^{144}Nd_{sample} -1) /0.1967)\Delta_{(t)})$, following De Paolo (1988).

3. Saint-Jean-du-Doigt Intrusive Complex (SJIC)

3.1. Geology

The Saint-Jean-du-Doigt Intrusion (SJIC) is located between the Trégor Cadomian domain, mainly composed of volcanoclastic formations overlying a Palaeoproterozoic (Icartian) gneissic basement (*c.* 2.0 Ga, Auvray et al., 1980), and the Léon Hercynian metamorphic domain (Fig. 1a). The SJIC is composite and includes four main units: the Primel cumulate-pegmatoid association, the Saint-Jean-du-Doigt monzogabbro-(Q-)monzonite mingled/mixed rocks, the Poul Rodou layered gabbro-diorites and several granitic bodies (Fig. 1b). Some doleritic dykes cross cut the units, but were not found in the granitic rocks. Most rocks have isotropic textures and exhibit no significant regional deformation subsequent to their emplacement, with the exception of local brittle faulting. However, they have undergone late- to post-magmatic alterations, resulting in the transformation of some primary minerals, without significant change in bulk rock chemistry (Coint et al., 2008). The SJIC was emplaced under a lithostatic pressure of about 0.5 GPa, i.e. at *c.* 15 km depth (amphibole geobarometry: Johnson and Rutherford, 1989 and Schmidt, 1992 *in* Coint et al., 2008), within Proterozoic rocks and Devonian-Carboniferous sediments. Chantraine et al. (1986) have reported a carboniferous U-Pb zircon age of *c.* 350 Ma for the gabbros (Deutsch, unpublished) confirmed by Barboni et al. (2008, 2010), who obtained U-Pb zircon ages at 347 ± 4 Ma for the mafic units and the granitic bodies from Poul Rodou. The SJIC was later intruded by red granites at *c.* 300 Ma (Fig. 1b). The SJIC mafic rocks have a tholeiitic affinity (Chantraine et al., 1986; Coint et al., 2008, 2009; see also section 5.2). Geochemical features of intermediate/felsic rocks are rather typical of calc-alkaline suites (Barboni et al., 2010; Capdevila, 2010).

3.2. Coastal SJIC from East to West

The Saint-Jean-du-Doigt Intrusive Complex is best exposed along the northern shoreline. Field observations have been made from Poul Rodou to Primel through the bay of Saint-Jean-du-Doigt (Fig. 1b).

3.2.1. Poul Rodou: gabbro-diorite layering

From southeast to northwest, the Poul Rodou cross-section begins with a small granitic body in sharp intrusive contact with a Proterozoic formation (Fig. 1b and 2a). The granite is equigranular and intrudes an intergranular/oikocrystic gabbro. Lobate contacts between the granite and the adjacent gabbro and gabbroic enclaves within the granite are interpreted as evidence for the contemporaneous crystallization of both magmas. Other granitic intrusions crop out along the shoreline, such as the Beg ar Fri granite (sample SJ22, Fig 1b and 2a). Several sub-parallel leucocratic sheets form layers within the gabbro. They are oriented SE-NW and dip slightly (10° to 30°) toward the northeast. They are cut southeastward by the granitic intrusion (Fig. 2a). This demonstrates the lack of apparent direct link between leucocratic sheets and granitic bodies. Leucocratic sheets are thin (a few decimeters thick) and sparse near the edge of the complex. They become thicker (up to several decimeters) and more abundant to the northwest. The spacing from one sheet to another varies from several decameters to a few meters. The upper contact with the overlying gabbro is systematically undulated, sometimes connected to felsic masses, a few decimeters in size, within the overlying gabbro (Fig. 3a, b). When elongated, these structures are orientated sub-perpendicularly to the sheet layers. They are interpreted as gravity-driven felsic diapirs extracted from the sheets. In the present orientation, these instabilities are not sub-vertical and the sheets are not sub-horizontal. The variable dipping angles of the structures along the Poul Rodou shoreline are consistent with post-emplacement brittle deformation and denotes northeastward tilting of blocks limited by NE-SW faults (Fig. 2a). The composition of the

leucocratic sheets is dioritic, with the exception of their upper part, sometimes Q-monzonitic (Table 1). All are moderately cumulative in plagioclase (cumulus from 20% at the base to 50% at the top of the sheets) and generally exhibit an intergranular texture. Felspar-rich (plagioclase and orthoclase) diapirs, more differentiated than their related sheets, have textures ranging from intergranular to pegmatitic. Contrasting with the upper contacts, bases of the leucocratic sheets form relatively regular surfaces with the underlying gabbro. Some sheets are connected from below to sub-perpendicular pipe-like feeding structures (Fig. 3b and c). In addition, when diapirs came near an overlying sheet, they could merge with it. Alternatively, some diapirs did not intersect the overlying sheet but formed concave-down structures (Fig. 3d). Except near Beg ar Fri, where an amphibole-rich cumulate has been sampled (SJ44b, Fig. 2a), the gabbro is structurally and texturally homogeneous throughout the Poul Rodou shoreline: no chilled margins, macrorhythmic units, or upward petrographic gradation were observed.

3.2.2. Saint-Jean's bay: monzogabbro-monzonite interactions

The coast north of Saint-Jean-du-Doigt exposes spectacular and various monzogabbro-(Q-)monzonite (see section 3.3 for rock nomenclature) interaction structures resulting from brittle brecciation to mixing (producing hybrid rocks) through mingling (during which the magmatic end-members retain their identity). At Saint-Jean's bay, angular breccias are present only east of the dextral fault *F* (Fig. 1b) whereas mingling/mixing predominates westward. Lobate structures are also visible in the transition zone to the Poul Rodou layered gabbro-diorite unit.

Structures that result from ductile interactions between coexisting magmas include pillowed mafic enclaves with chilled margins enclosed in a heterogeneous monzogabbro (mingling, Fig. 4a), hybrid magmas (pure mixing), and banded rocks in the process of

hybridization (mingling/mixing, Fig. 4b). In partly hybridized rocks, several mafic enclaves show diffuse margins. These interactions can be observed from microscopic (less than one millimeter) to outcrop scales (several tens of meters). Locally, mafic enclaves present a N40°E preferred orientation, suggesting ductile deformation in protoshear zones.

The angular facies consist of jigsaw-type breccias where polyhedral mafic enclaves are enclosed in intermediate rocks forming a vein network (Fig. 4c). The veins are texturally homogeneous intergranular (Q-)monzonites whereas a few blocky clasts exhibit mixing/mingling features.

3.2.3. Primel: cumulate-pegmatoid association

Pegmatoids (gabbroic pegmatites), generally associated with plagioclase-phyric cumulates, are distributed from Roc'h Louet to Primel (Fig. 1b). Cumulates are well exposed at Roc'h Louet (Fig. 2b), whereas the coarsest-grained pegmatoid, containing large amphibole crystals (up to 15 centimeters in length) and smaller plagioclase crystals, occurs westward near the Primel red granite (Fig. 2c). There, pegmatoids occur as pods or veins within mafic heteradcumulates with variable plagioclase contents. They are sometimes zoned, with an amphibole-richer core. Pegmatoids are often more altered than the host gabbro. The cumulate-pegmatoid association is bordered southward and southeastward by the monzogabbro-(Q-)monzonite unit of Saint-Jean. In this area, monzogabbros are locally rich in feldspar megacrysts, similar to those described by Wiebe and Collins (1998) and Collins et al. (2006) in the Devonian Kameruka Granodiorite (Bega batholith, southeastern Australia). Fine-grained pegmatoids are found as patches or thin veins in mingled monzogabbro-(Q-)monzonite at Saint-Jean's bay western edge (Fig. 2b). In this zone, mottled pegmatoids have also been observed. They are characterized by recrystallized amphibole-bearing flecks from 2 to 5 cm in diameter (see section 3.3).

218 Gabbroic aplites are often intimately associated with pegmatoids as patches or
219 irregular veinlets (Fig. 4d). They are distinct from the doleritic dykes, which display sharp
220 intrusive contacts with host rocks and have chilled margins.
221 In sample PM2 (Fig. 4d), an aplitic vein separates the pegmatoid from the cumulate,
222 the latter being edged by a dark reaction zone.
223
224 *3.3. Petrology*
225
226 According to the recommendations of the IUGS, the nomenclature of plutonic rocks is
227 based on modal compositions. As not all the primary phases are preserved, we have chosen to
228 use the R1-R2 chemical discrimination diagrams of La Roche et al. (1980), as utilized by
229 many authors (e.g., López-Moro and López-Plaza, 2004; Hellström et al., 2004).
230 At Poul Rodou, the SJIC rocks plot within the following fields of a R1-R2 diagram:
231 olivine gabbro; diorite, monzodiorite and (Q-)monzonite (sheets and diapirs); and granite
232 (intrusions). The Saint-Jean's bay samples plot as follow: olivine gabbro (doleritic dykes);
233 monzogabbro, monzonite, and Q-monzonite (mixing/mingling facies). At Primel, pegmatoids
234 are olivine gabbros. Associated cumulates plot as pyroxenite, a term not used here, given the
235 lack of modal pyroxene in the rocks. Following a similar line of argument (lack of olivine),
236 we prefer the term "gabbro" to "olivine gabbro".
237 The Primel cumulates mainly enclose labradorite, secondarily albitized, as a cumulus
238 phase (from 30 to 65 vol. %), with interstitial actinolite (which replaces oikocrysts, probably
239 of pyroxene), Fe-Ti oxides and apatite.
240 Pegmatoids are mainly composed of skeletal green hornblende and elongated albitized
241 plagioclase. Relics of diopside have been identified in a few samples. Small comb-shaped Fe-
242 Ti oxides, biotite and acicular apatite fill the spaces between the large crystals. The flecks of

243 the mottled pegmatoids on the western edge of Saint-Jean's bay contain Fe-Ti oxides,
244 amphibole and phyllosilicates. They might result from recrystallization of ancient oikocrystic
245 pyroxenes.

246 Gabbros and monzogabbros from the SJIC contain saussuritized plagioclase laths,
247 green hornblende, acicular actinolite, Fe-Ti oxides, apatite, biotite and sparse titanite and
248 zircon. Large oikocrysts of brown hornblende have been identified in several monzogabbro
249 samples. The dolerites are fine-grained and have a typical greenschist facies mineral
250 assemblage (albite, actinolite, epidote, chlorite).

251 The SJIC (Q-)monzonites are especially rich in andesine (up to 75 vol. %). The main
252 ferro-magnesian mineral is actinolite. The Q-monzonites, which are mainly located east of
253 Saint-Jean's bay, have more than 10 vol. % of quartz. Sheets and diapirs from the SJIC range
254 from diorite to Q-monzonite in composition. Sheets are rich in albitic plagioclase but also
255 contain amphibole (green hornblende and actinolite) with variable amounts of interstitial
256 quartz. Diapirs contain quartz, plagioclase, K-felspar and epidote.

257 Granites contain orthoclase, quartz, plagioclase, biotite, apatite and rare zircons.
258 Symplectitic quartz-feldspar associations are present in many SJIC granitic samples
259 (myrmekite).

260

261 **4. North-Guernsey Intrusive Complex (NGIC)**

262

263 *4.1. Geology*

264

265 Guernsey (Channel Islands), about 50 km off the French coast, is part of the
266 Armorican Massif (Fig. 1a). The island is divided into two main geological domains. The
267 Southern Metamorphic Complex mainly consists of Palaeoproterozoic gneisses (including the

268 Icart orthogneiss, with a magmatic U-Pb/zircon age of 2061 ± 2 Ma, Samson and D'Lemos,
269 1998), which were later intruded by the deformed Neoproterozoic Perelle Q-diorite (Samson
270 and D'Lemos, 1999). The Northern Neoproterozoic Intrusive Complex – hereafter referred to
271 as the North-Guernsey Intrusive Complex (NGIC) – is undeformed and partly composed of
272 layered rocks (Elwell et al., 1960, 1962; Bremond d'Ars, 1990; Bremond d'Ars et al., 1992).
273 The composite NGIC consists of four distinct units: the Saint Peter Port gabbro, the gabbro-
274 dioritic Bordeaux Group, the L'Ancresse granodiorite and the Cobo granite (Topley et al.,
275 1990; Fig. 1c). All these plutonic units were emplaced at the end of the Cadomian orogeny, at
276 about 560-550 Ma (Bremond d'Ars et al., 1992). The present study mainly deals with gabbro-
277 diorite layering in the Bordeaux Group (the Beaucette type in Bremond d'Ars et al., 1992) and
278 with the Spur Point cumulate-pegmatoid association (Saint Peter Port Gabbro). Alteration of
279 the NGIC rocks is generally moderate. Petrologic studies indicate that the Saint Peter Port
280 gabbro was emplaced under a lithostatic pressure of about 0.4 GPa (*c.* 12 km depth),
281 amphibole and plagioclase crystallized at about 940°C under relatively high oxygen fugacity
282 conditions, and magma water content ranged from 2 to 6 wt% (Bremond d'Ars et al., 1992).
283 The complex has a calc-alkaline affinity (Bremond d'Ars et al., 1992; see also section 5.2)
284 and belongs to the M-type Cadomian Granitoid Belt of Graviou and Auvray (1985).
285
286 *4.2. NGIC layering*
287
288 *4.2.1. Beaucette Marina: veined gabbroic macrorhythms*
289 The outcrops of the Beaucette Marina (gabbro-dioritic Bordeaux Group) show
290 partially cumulative macrorhythmic sequences, which are less than one to several meters
291 thick, and dip 20° westward (Fig. 2d, e and 5a, b, c). They are locally intruded by doleritic or
292 dioritic dykes. Each macrorhythm is composed of a gabbroic unit overlying a melagabbroic

unit. The base of a melagabbroic unit is generally fine-grained, as also observed by Elwell et al. (1960). The transition from a melagabbroic unit to an overlying gabbroic one is gradational, with amounts of phyric amphiboles decreasing upwards (see Fig. 9 insets in section 5.1). Both units have an orthocumulate texture. While melagabbroic units are petrologically homogeneous, the main gabbroic unit is formed by alternating dark and mesocratic layers of a few centimeters thick (Fig. 5c) and is veined by leucocratic material, forming an inter- and cross-connected network of centimeter-thick sheets, broadly parallel to the layering (Fig. 5d).

Immediately below some melagabbroic units, thick evolved-gabbroic sheets are observed, from which leucocratic pipes protrude upwards into the overlying melagabbros (Fig. 5a, b). Such pipe-producing sheets also occur, more rarely, in the interior of the melagabbroic units (Fig. 5a). They have a texture ranging from intergranular to orthocumulative. The upper limit of the evolved-gabbroic sheets is irregular, sometimes diffuse. Elwell et al. (1960) has described fine-grained margins in the upper part of some gabbroic units at the contact with the pipe-producing sheets. All the leucocratic pipes are inclined on average at about 30° from the main layering (Fig. 5e). They plunge toward the S-SE. North of the area shown in Fig. 2e, two generations of neighboring pipes have distinct pitches (*c.* 10° and 40° from the layering). Pipe compositions range from monzodiorite (this study) to granodiorite (Elwell et al., 1960). In cross-section, the pipes are zoned, the core being less differentiated than the rim (Fig. 5f; Elwell et al., 1960). The upper part of the pipes is pegmatitic and the host rocks are systematically altered near the pegmatitic zones (Fig. 5f). Elwell et al. (1960) have described two spots where pipes join with the overlying cross-connected dioritic vein system.

4.2.2. Spur Point: cumulate-pegmatoid association

The Saint Peter Port gabbro is a 0.8 km-thick layered slab, gently dipping westward (Briden et al., 1982). It is composed of three main rock types (Bremond d'Ars et al., 1992). The most spectacular of which is the mottled orthocumulate of Spur Point, characterized by layers of poikilitic amphibole crystal flecks (Roach, 1971; Bremond d'Ars, 1990; Bremond d'Ars et al, 1992; Fig. 6a, b). This facies has been interpreted as a boundary layer cumulate (Bremond d'Ars et al, 1992).

Pegmatoidic rocks crop out at Spur Point (Fig. 6c). Their mineralogy and texture are similar to those in the SJIC. However, here in the NGIC, cumulates associated with pegmatoids are mottled.

4.3. Petrology

In a R1-R2 diagram (La Roche et al., 1980), Beaucette's rocks are gabbronorite (melagabbroic units), olivine gabbro (gabbroic units and pipe-producing sheets), diorite (dykes and cross-connected veins), and monzodiorite (pipes). As for Primel (SJIC), the Spur Point cumulates plot as pyroxenite, a term not used here.

The Spur Point mottled orthocumulates contain cumulus calcic plagioclase (An 80) and clinopyroxene (Fig. 6b). The intercumulus phases are clino- and orthopyroxene, amphibole (hastingsite), Fe-Ti oxides and apatite. The flecks correspond to large oikocrystic amphiboles.

The NGIC pegmatoids are composed of large skeletal green hornblende, elongate albitized plagioclase, comb-shaped Fe-Ti oxides, biotite and acicular apatite.

Gabbroic and granitic rocks have also mineralogies comparable to those of the SJIC gabbros and granites. The melagabbros (gabbronorites) show green hornblende as cumulus

342 phase (< 50 vol. %), as well as plagioclase, Fe-Ti oxides, apatite and biotite. We have also
343 noted the presence of clots of small amphibole grains in these rocks.
344 In Beaucette, the dioritic veins, sheets and dykes are mainly composed of plagioclase,
345 hornblende and biotite, whereas the monzo/granodioritic pipes are rich in plagioclase, K-
346 felspar, green hornblende and, occasionally, quartz and clinopyroxene. The sheet sample
347 GS13a is composed of *c.* 30 % of 2 mm-long zoned plagioclase, as cumulus phase.
348 Concentrations of acicular hornblende are observed where pipes connect overlying cross-
349 connected dioritic veins (Elwell et al., 1960).
350 The pipe-producing evolved gabbroic sheet sample GS13a from Beaucette and the
351 mottled orthocumulate sample GS1a from Spur Point are both characterized by cumulus An-
352 rich plagioclase (An 60-90: Fig. 7a). No other analyzed NGIC sample shows such a
353 characteristic. A chemical profile across such a plagioclase crystal (sample GS1a, Fig. 7b)
354 reveals a calcic mantle (An 60-75) comprised between an An-rich core (An 75-90) and an An-
355 poor margin (An 40-55). This mineralogical specificity will be discussed in section 6.3.1.
356
357 **5. Geochemistry**
358
359 *5.1. Geochemical sections through gabbro-diorite units*
360
361 Vertical variations of MgO, TiO_2 and Al_2O_3 through four gabbro-dioritic sections are
362 shown in Figs 8 (SJIC) and 9 (NGIC). The chemical composition of the Poul Rodou gabbro is
363 relatively constant, above and below the diapir-producing leucocratic sheets, for all the
364 sections (Fig. 8). Only TiO_2 varies significantly, from 1.18 (SJ34g) to 1.91 wt% (SJ43f). This
365 relative chemical homogeneity of the mafic body is a rather original feature with respect to
366 many other MASLIs (e.g., Wiebe, 1996). By contrast, the macrorhythmic sequences of the

NGIC display variable compositions (Fig. 9). Melagabbros are highly magnesian, with MgO contents up to 14.35 wt% (GS10d). MgO is slightly higher in the lower part of the melagabbroic units (GS7a versus GS7d in Fig. 9). Gabbroic units are more heterogeneous and less magnesian (5 < MgO < 10 wt%, Fig. 9). The leucocratic veins, sheets and diapirs/pipes display various compositions. In both intrusions, the diapirs/pipes are systematically more evolved than the sheets from which they are extracted (SJ34b1 versus SJ34c; GS10c versus GS13a; Table 1 and Figs 8 and 9). However, parts of some sheets are more differentiated than some diapirs. For example, the upper part of the sheet SJ43c is more evolved than the diapir SJ34b1, which relates to another sheet (Table 1 and Fig. 8).

5.2. Trace elements

Trace elements which are both incompatible and immobile can be used to determine the magmatic affinity of the mafic rocks. In the La/10-Y/15-Nb/8 diagram (Fig. 10) of Cabanis and Lecolle (1989), the SJIC gabbros and monzogabbros plot mainly in the E-MORB field whereas the gabbros and melagabbros from the NGIC clearly have a calc-alkaline affinity.

The chondrite-normalized rare earth element (REE) field of the Poul Rodou gabbros (SJIC) is shown in Fig. 11a, with REE patterns of two leucocratic sheets and related diapirs. The sheet and diapir SJ34 are moderately differentiated. The diapir SJ34b1 is slightly enriched in light REE (LREE) and depleted in heavy REE (HREE) with respect to the corresponding sheet SJ34c, which plots above the gabbroic field. The sheet sample SJ43c shows lower REE concentrations than the less differentiated sheet sample SJ34c. The diapir SJ43d is enriched in LREE and depleted in HREE with respect to its parental sheet SJ43c. Both have positive Eu anomalies.

392 The REE patterns of some other rocks representative of the SJIC are exhibited in Fig.
393 11b. Pattern similarities between the diapir SJ34b1 and the monzonite SJ9 (mingling zone at
394 Saint-Jean's bay) and between the evolved sheet SJ43c and the Q-monzonite SJ17 (vein in
395 breccia with angular clasts at Saint-Jean's bay) are noticeable. The pegmatoid SJ16 is less rich
396 in REE than the gabbros. Of all the samples, cumulates have the lowest REE contents. With
397 respect to the monzonite SJ9, the granite SJ22 is enriched in Ce and HREE, and displays a
398 large negative Eu anomaly.

399 In the NGIC, all the samples from the macrorhythmic sequences have parallel patterns
400 (Fig. 11c). This is also the case for the pipe-producing gabbroic sheet GS13a, located near the
401 upper limit of the gabbroic REE field. By contrast, the thin dioritic sheet GS7c and the
402 monzodioritic pipe GS10c are highly depleted in HREE with respect to GS13a. Although
403 contents of La, Eu and Yb are equal in GS10c and GS7c, GS10c has a concave-up shaped
404 pattern indicating depletion in Middle REE (with the exception of Eu).

405 The gabbroic pipe-producing sheet GS13a and the mottled cumulate of Spur Point
406 GS1a, which contain An-rich plagioclase phenocrysts (An 60-90: Fig. 7), display cross-
407 cutting REE curves, with comparable Eu contents (Fig. 11d). The Cobo granite GS8 has a
408 concave-up pattern and a negative Eu anomaly.

409

410 *5.3. Isotopes*

411

412 The Sr and Nd isotopic data and analytic details are shown in Table 2. The range of
413 the NGIC $^{87}Sr/^{86}Sr$ initial ratios is very restricted (0.7055 to 0.7058), regardless of the rock
414 type (data from Bremond d'Ars et al., 1992). In the SJIC, mafic rocks (gabbros, pegmatoids,
415 and dolerites) exhibit the most positive εt_{Nd} values at 347 Ma (+4.7 to 5.9) and initial Sr ratios
416 between 0.7039 and 0.7049. These values are similar to those obtained by Barboni et al.

417 (2010) on pseudo-adakites related to the SJIC (+2.9 to + 6.8 and 0.7038 to 0.7047). The
418 intermediate SJIC rocks (monzogabbros, monzonites, Q-monzonites, and diorite) have less
419 positive εt_{Nd} values (+2.4 to +3.2) and initial Sr ratios which range from 0.7043 to 0.7069.
420 This scattering suggests that the Rb-Sr system was not closed. The granite sample SJ22 also
421 exhibits a positive εt_{Nd} value at 347 Ma (+3.0) and a low initial Sr ratio (<0.700) which also
422 shows open system behavior for Rb-Sr. A noticeable feature is the sharp isotopic contrast
423 between the Poul Rodou gabbro SJ34a (+5.9) and the dioritic sheet SJ34c (+2.6), two
424 neighbor samples separated by *c.* 3 m (Fig. 3a and 8).
425 It follows that the gabbro and the leucocratic sheets from Poul Rodou are not
426 cogenetic. The source of the former corresponds to that of the doleritic dykes and peripheral
427 pegmatoids, whereas the Poul Rodou sheets (and diapirs) have an isotopic composition
428 comparable to that of the other SJIC intermediate rocks.
429
430 **6. Discussion**
431
432 *6.1. A review*
433
434 *6.1.1. MASLI-type reservoirs: the models*
435 Wiebe and others have defined the concept of MASLI and studied many examples of
436 such intrusions, especially in Maine. A MASLI petrologically corresponds to a composite
437 layered sequence of alternating gabbroic and dioritic units situated between or below granitic
438 bodies (Chapman and Rhodes, 1992; Wiebe, 1996; Wiebe and Collins, 1998). Variants are
439 intrusions of bimodal gabbro-diorite (e.g., Ingonish, Cape Breton Island: Wiebe, 1974) or
440 diorite-granite (e.g., Nord-Forez, Massif Central, France: Barbarin, 1988), which display
441 some of the characteristic features of MASLIs. These complexes are interpreted to be the

result of repeated mafic intrusions in a crystallizing dioritic/granitic reservoir (Wiebe, 1974, 1993b, 1996). This group of models is supported, among other things, by the observation of pillow-like bodies of chilled gabbro in intermediate/felsic rocks (Wiebe, 1993b; Wiebe et al., 2001). Diorites are generally viewed either as products of fractional crystallization of the gabbro, or as resident cumulates.

A multistep model for the Isle au Haut Maine igneous complex (Maine), similar to those of Wiebe and others, was proposed by Chapman and Rhodes (1992). The model accounts for the formation of a layered sequence of ten alternating (tholeiitic) gabbroic and dioritic units of magmas, which were contemporaneous. The bases of the gabbros are chilled against the underlying diorites. The authors state that mafic liquids were periodically emplaced into a silicic magma chamber at the rheological transition from a relatively felsic cumulate to an overlying felsic magma. Each gabbroic unit is injected below a dioritic liquid, but above a solidifying dioritic crystal mush, as expected from the magma density contrast. Once emplaced, crystallization progresses in the underlying dioritic mush and produces Q-monzodioritic sheets and pipes, which intrude the gabbroic layer. Diapirs are subsequently produced from the crystallizing sheets.

The development of such gravity-driven instabilities in layered magmas have been modeled and applied to the NGIC (Bremond d'Ars, 1990; Bremond d'Ars and Davy, 1991). However, according to these authors, it is not clear whether the sheets in the NGIC result from intrusions within the gabbros, or the reverse. The opinion of Wiebe (1993b) is that "the 'veins' in Guernsey have textures and compositions that are appropriate for feldspar cumulates, not solidified liquids". He views the NGIC as a crystallizing intermediate/felsic reservoir periodically invaded by mafic liquids.

6.1.2. Cumulates and pegmatoids

The connection between mafic cumulates, gabbroic pegmatites (pegmatoids) and aplites has been established by many authors. For instance, Beard and Day (1986) published a thorough study of such rocks in the Smartville intrusive complex, Sierra Nevada, California. They pointed out the following features: (i) the pegmatoids occur as pods and segregations in gabbroic rocks; (ii) they are often found in association with fine-grained aplite of similar mineral assemblage; and (iii) they have a very mafic composition, as observed by other authors (e.g., McBirney and Noyes, 1979). Contrary to previous authors who proposed subsolidus processes (e.g., Bow et al., 1982), Beard and Day (1986) favour that rocks form by *in situ* crystallization. They envisage that a mafic intercumulus melt is extracted from a cumulate stack in the presence of a fluid phase. The process could be enhanced by the disruption of the cumulate assemblage due to a drop in the confining pressure. This model is consistent with the one proposed by Momme and Wilson (2002) for the Kraemer Island macrodyke, Greenland. It is also similar to the model of pegmatoid formation in thick basaltic lava flows proposed by Caroff et al. (1997). An alternative model suggests that the pegmatoid crystals grew by reaction between primary mafic mineral grains and a superheated liquid possibly resulting from a pressure drop (Cawthorn and Boerst, 2006). In a plumbing system connected to the surface, a pressure drop can easily be achieved subsequent to an eruption. In an intrusion, confined at depth within deformable host rocks, only a volumetric expansion of a constant mass plumbing system could also induce a pressure drop.

6.2. Layering and diapirism in the SJIC and NGIC

Both SJIC and NGIC display comparable characteristics, which justifies the present combined study: (1) both intrusions are triple-component MASLIs (gabbro, diorite and granite); (2) pegmatoids occur in association with mafic cumulates, especially at the edges of

both complexes; (3) a lateral or basal part of the intrusions is formed by gabbroic sequences interlayered with dioritic sheets producing diapirs. Nevertheless, numerous contrasted features lead us to propose two different models for the construction of the gabbro-dioritic layered sequences.

6.2.1. Melagabbros and gabbros

Two noticeable features of the NGIC gabbro-dioritic unit not observed in the SJIC are the presence of macrorhythms and modal layering within the gabbroic sequences. This petrological heterogeneity induces geochemical variations (Fig. 9 and 11c) and suggests crystal accumulation. By contrast, the tholeiitic Poul Rodou gabbro (SJIC) is relatively homogeneous (Fig. 11a). Therefore, it is probably not a cumulate, but was rather a liquid that crystallized *in situ* without significant crystal settling, possibly after a period of convection. For instance, Philpotts et al. (1996) have shown that tholeiitic magmas, when only one-third crystallized, can form crystal mushes dominated by thin laths of plagioclase and elongated pyroxene grains. In such magmas, an interlocking network of crystals can form at low solid content (possibly only 20%), precluding any further convection and crystal settling. Such a model is consistent with both the tholeiitic affinity of the Saint-Jean gabbro (Fig. 10) and the rock textures, which are intergranular to oikocrystic. On the contrary, the rhythmic sequences of the calc-alkaline NGIC, and the orthocumulate texture fit with a crystal accumulation model.

In Fig. 12, we propose two models to explain the formation of the gabbro-dioritic layered sections of the SJIC and NGIC. The Poul Rodou gabbro is purported to be a simple network-type crystal mush, crystallizing from the base up (Fig. 12a, b, c). In Beaucette, each melagabbro/gabbro pair is asserted to correspond to a mafic recharge (Fig. 12d, g), having undergone two successive crystal-settling events. At first, settling involves only mafic crystals

517 (olivine, pyroxene ± primary hornblende: Fig. 12e) and next, plagioclase appears on the
518 liquidus (Fig. 12f). In the first step, densities of the mafic crystals are comparable and the
519 resulting cumulate is highly mafic and texturally homogeneous (melagabbroic unit). With the
520 appearance of plagioclase, the density difference between feldspar and mafic crystals can
521 produce alternating dark/mesocratic layers (gabbroic unit), according to the model of Sparks
522 et al. (1993).
523
524 *6.2.2. Formation of leucocratic sheets and diapirs*
525 Models of dioritic/monzonitic reservoirs periodically replenished by mafic liquids
526 hardly apply to all the stages of construction of both intrusions.
527 *In the SJIC*, observations supporting the idea that intermediate magmas have invaded
528 mafic ones include: (1) the several sheets of intermediate composition that we interpret as
529 intrusions in the Poul Rodou homogeneous gabbro; (2) the monzonitic dykes throughout most
530 of Saint-Jean's bay, especially those including angular mafic breccias (Fig. 4c); (3) the lack of
531 evidence for chilling of the Poul Rodou gabbro against the dioritic sheets (Fig. 8); and (4) the
532 large predominance of the gabbroic rocks over the whole intrusion. We do not exclude that
533 mafic inputs, at huge rates, possibly inducing intensive thermal rejuvenation of a more felsic
534 resident magma, were previously involved in the SJIC. We mean here that, as observed today,
535 (1) and (2) are unlikely the direct, *in situ* or slightly displaced, remnants of an initial felsic
536 reservoir that remains rather hypothetical from (3) and (4).
537 The chilled gabbroic pillow-like enclaves, such as those of Fig. 4a, result from
538 fragmentation of mafic magmas in more felsic ones. Such a mingling is controlled by
539 rheological contrasts and/or surface energy and depends on the relative volumes and
540 temperatures of available magmas (e.g., Sparks and Marshall, 1986; Fernandez and Barbarin,
541 1991; Hallot et al., 1996; Pons et al., 2006). Thus, it can be achieved during or just after new

mafic inputs, but may alternatively result from convective motions in the interior of a large composite reservoir or from injections of an external more felsic magma into a resident mafic magma. Chilling of the latter just requires significant volumes of colder, but still mobile, more felsic magmas.

Therefore, we propose a model of a reservoir repeatedly replenished by dioritic magmas for the SJIC. Those magmas were not genetically related, nor had they to be initially at the same temperature. In the reservoir, the gabbroic magma density increases downward with cooling, hence crystallinity. Andesites/diorites and basalts/gabbros may have comparable densities, especially when they are of tholeiitic affinity (e.g., Sparks et al., 1980; Sparks and Huppert, 1984; Caroff, 1995). A partly crystallized dioritic magma rising through a tholeiitic gabbro crystallizing from below is thus expected to be buoyant initially, then at neutral buoyancy and finally denser than the gabbroic magma. In Fig 12a and b, a 950°C dioritic magma with 30% plagioclase phenocrysts enters a gabbroic reservoir crystallizing from below. At the base (1), the gabbroic magma is 70% solid at 1100°C. At upper levels (2) and (3), it is 30% solid at 1150°C and liquid at 1200°C, respectively (all values are approximates). Reaction kinetics being much slower than heat transfer, a metastable dioritic melt plus crystals at thermal equilibrium with the resident magma is considered at these levels. Densities were estimated given that the density of a liquid, obtained from Bottinga and Weill (1970), is about 90% of that of its solid equivalent and assuming that this ratio applies to the solid fraction whatever it is (Fig. 12). The results show that at levels (1) and (2), a gabbroic magma remains denser than a dioritic magma. At level (3), equidensity is reached allowing a dioritic magma to spread out, forming sheets. Thus, we interpret each SJIC sheet as the result of some horizontal emplacement of porphyric magmas of intermediate composition into poorly crystallized gabbros at levels of neutral buoyancy. Late felsic diapirs formed at the top of emplaced sheets while the equidensity front moved upward as cooling proceeded (Fig. 12b

and c). *In situ* fractionation within the sheets favored the late production of low density magmatic liquids. The REE patterns of the diapirs are depleted in HREE with respect to the sheets from which they were extracted (Fig. 11a). This is consistent with fractionation of a significant amount of amphibole within the sheets. Indeed, amphibole preferentially incorporates middle to heavy REE relative to LREE (e.g., Caroff et al., 1999).

In the NGIC, dioritic sheet and vein geometries are controlled by the macrorhythms: the pipe-producing sheets are generally located along the lower boundary of the melagabbroic units and the cross-connected dioritic vein network forms in the gabbroic units according to the framework of the dark/mesocratic layers. These features suggest that the gabbroic structures existed prior to the dioritic veining. The fine-grained margins at the base of melagabbroic units relate to mafic replenishments before the dioritic invasion.

The main similarity between the SJIC and the NGIC was the late influx of the dioritic magmas with respect to the main gabbroic magmas. At Beaucette, both magmas were close to isotopic equilibrium. The emplacement of the dioritic sheets was not directly controlled by density ratios, but rather by pre-existent rhythmic structures within cumulates (Fig. 12h). Two groups of sheets have to be distinguished. An initial gabbroic to dioritic magma was emplaced just beneath the base of the melagabbroic units (Fig. 5a, c). The sheet-derived pipes cut across the melagabbroic unit (Fig. 5b), until the overlying gabbroic unit. The concave-up shape of the REE pattern of the pipe GS10c (Fig. 11c) is consistent with crystallization and fractionation of both amphibole and apatite in its parental sheet (Caroff et al., 1999). Relative motions between the unconsolidated/mushy units possibly caused the vertical pipes to become inclined (Fig. 5e, 12i), as previously proposed by Elwell et al. (1960). They might have created proto-fissures in the gabbroic unit and thus have favored the emplacement of the (monzo)dioritic second group of sheets, which are cross-connected and fed by the pipes (Fig. 5d, 12i). The gabbroic layering, seen as controlling the architecture of the cross-connected

592 vein/sheet network, supports our interpretation of late dioritic invasion within gabbros.
593 Cumulative features of the sheets reveal that the invading magmas possibly contained
594 plagioclase phenocrysts, such as those in the SJIC.
595
596 *6.3. Variations in the mode of MASLI construction*
597
598 Our models (Fig. 12) agree with the general physical conditions and the mechanisms
599 by which layers, pipes, diapirs and other plutonic structures are supposed to form within
600 crystallizing magmas (e.g., see Barbey, 2009 and Patterson, 2009 and references therein for
601 recent reviews). In our opinion, the SJIC and the NGIC support the general idea that
602 intermediate/felsic replenishment of a mafic reservoir is a situation much more common than
603 previously thought, though not as common as mafic replenishment.
604
605 *6.3.1. NGIC*
606 Bremond d'Ars et al. (1992) have proposed a sketchy model of the NGIC reservoir.
607 According to these authors, the layered rocks (Saint-Peter Port cumulate and Beaucette-type
608 gabbro-diorite) formed near the margin of the chamber, by upwards prograding crystallization
609 and replenishments. The present dip of the layers is primary. Far from the margins, the centre
610 of the reservoir was probably convective, which explains the lack of layering in most of the
611 Bordeaux gabbro-diorite outcrops, with the exception of Beaucette. The peripheral granitic
612 bodies (Cobo, L'Ancresse) are proposed to form by mixing and assimilation of crust-derived
613 melts with the gabbro-diorite magmas. Large volumes of mafic magma are thought to have
614 induced melting of country rocks at depth within the plumbing system.
615 We agree with the basic ideas of this model, except for the the hypothesis of crustal
616 melting. Although interactions between gabbro-dioritic and granitic rocks are undeniable

617 (Topley et al., 1982; D'Lemos, 1996), available isotopic data seems hardly consistent with
618 crustal melting (Table 2). We rather suggest, as D'Lemos (1996), that at least the Cobo
619 granite is to a great extent cogenetic with the Bordeaux gabbro-diorite, as it is often observed
620 in MASLIs (e.g., Wiebe, 1993a, b, 1994, 1996; Wiebe and Collins, 1998).

621 An-rich plagioclases in both the mottled cumulate GS1a from Spur Point and the
622 gabbroic sheet sample GS13a from Beaucette support the hypothesis that the invading dioritic
623 liquid(s) originate(s) from the mottled Saint-Peter-Port/Spur Point cumulate, interpreted as a
624 boundary layer by Bremond d'Ars et al. (1992). An-rich plagioclase cores (An>75, Fig. 7b)
625 suggest crystallization under hydrous conditions (Cordier et al., 2007). Derivation of a
626 GS13a-type composition from a liquid leaving a GS1a-type cumulate is also supported by
627 trace element compositions. Indeed, cross-cutting REE curves in Fig. 11d possibly reflect
628 crystal fractionation/accumulation (plagioclase, amphibole and/or apatite).

629

630 *6.3.2. SJIC*

631 A model of the SJIC is drawn in Fig. 13.

632 Granitic intrusions (Fig. 2a) have emplaced during or just after the crystallization of
633 the gabbro-dioritic magmas.

634 Pegmatoids and associated mafic cumulates are located near the edge of the complex
635 (Fig. 1b and 2b, c). With an isotopic composition close to that of the Poul Rodou gabbro and
636 the doleritic dykes, but more mafic, pegmatoids likely correspond to liquids issued from a
637 mafic intercumulus melt in the presence of a fluid phase. Melt extraction might have been
638 enhanced by the disruption of the cumulate stack, perhaps in a context of drop of the
639 confining pressure (Beard and Day, 1986; Momme and Wilson, 2002). Reactions of the liquid
640 with primary mafic minerals of the cumulate might explain Mg-rich pegmatoid compositions
641 (Cawthorn and Boerst, 2006).

642 Mixing and mingling seem to have preferentially occurred in the central part of the
643 reservoir. Dioritic liquids (in a broad sense) mix with gabbroic magmas to form variable
644 hybridized products, the isotopic composition of which tends toward that of the diorites. The
645 most homogeneous hybridized product, which has a dioritic isotopic signature (Table 2),
646 corresponds to the Saint-Jean's bay monzogabbro. Such an isotopic homogenization in a
647 MASLI, by mixing and diffusion (Steward and De Paolo, 1992), has already been described
648 by Waight et al. (2007). Angular breccias, also drawn in Fig. 13, can result either from
649 gabbro/diorite interactions in a more peripheral (i.e. colder) region of the reservoir, or,
650 alternatively, from late arrivals of dioritic liquids in a solidifying magma. The ductile to brittle
651 behavior of a magma which can be inferred from the preserved shapes of the enclaves also
652 depends on the strain rates involved during fragmentation (Fernandez and Gasquet, 1994;
653 Hallot et al., 1996; Petford, 2009).
654 At Poul Rodou, the isotopic composition of the felsic sheets differs from that of the
655 enclosing resident gabbro. The SJIC intermediate and felsic products are therefore issued
656 from a source which is different from that of the Poul Rodou gabbro / Primel pegmatoid /
657 Saint-Jean dolerite group. An AFC-type crustal contamination of the felsic liquid in a deep
658 reservoir possibly accounts for such features.
659
660 **7. Conclusions**
661
662 (1) The Saint-Jean-du-Doigt (SJIC) and the North-Guernsey (NGIC) Intrusive
663 Complexes are two MAfic-Silicic Layered Intrusions (MASLI) of the armorican Massif. Both
664 are triple component complexes (gabbro, diorite, granite) characterized by the occurrence of
665 pegmatoids in association with cumulates and of gabbroic units including diapir-producing

dioritic sheets. The NGIC is Cadomian and calc-alkaline. Mafic rocks of the Hercynian SJIC are tholeiitic.

(2) Pegmatoids are interpreted as liquids extracted from a mafic intercumulus melt in the presence of a fluid phase, subsequent to the disruption of a peripheral cumulate stack, possibly during a drop of the confining pressure.

(3) At least at some stages, the gabbro-dioritic units of the SJIC and the NGIC can both result from repeated influxes of magmas of intermediate composition within mafic reservoirs, but they are built differently. The SJIC gabbro could result from *in situ* crystallization of a relatively uniform magma in which crystal settling was not significant. Assuming they were metastable, dioritic magmas could have risen as gravity-driven diapirs in such a crystallizing gabbro before they spread to form sheets at levels of neutral buoyancy. By contrast, the NGIC gabbros correspond to cumulates. At Beaucette, they display a rhythmic layering which has guided the subsequent dioritic injections.

Acknowledgements

We are grateful to P.-M. Le Dantec for field assistance (Primel and Roc'h Louet cartography). Detailed and constructive comments by Dr P. Barbey and an anonymous reviewer helped us to improve the manuscript. Pertinent suggestions of A. Brink are gratefully acknowledged. We also thank Dr C.G. Barnes for discussions and Dr N. Eby for editorial assistance.

References

Auvray, B., Charlot, R., Vidal, P., 1980. Données nouvelles sur le protérozoïque inférieur du domaine nord-armoricain (France) : âge et signification. Canadian Journal of Earth Sciences 17, 532-538.

Barbarin, B., 1988. Field evidence for successive mixing and mingling between the Piolard Diorite and the Saint-Julien-la-Vêtre Monzogranite (Nord-Forez, Massif Central, France). Canadian Journal of Earth Sciences 25, 49-59.

Barbey, P., 2009. Layering and schlieren in granitoids: a record of interactions between magma emplacement, crystallization and deformation in growing plutons. Geologica Belgica 12, 109-133.

Barboni, M., Bussy, F., Schoene, B., Schaltegger, U., 2008. Architecture and emplacement mechanism of the Saint Jean du Doigt bimodal intrusion, Brittany, France. Geophys. Res. Abstr. 10, EGU2008-A-05182.

Barboni, M., Bussy, F., Chiaradia, M., 2010. Origin of Early Carboniferous pseudo-adakites in northern Brittany (France) through massive amphibole fractionation from hydrous basalt. Terra Nova, doi:10.1111/j.1365-3121.2010.00974.x.

Beard, J.S., Day, H.W., 1986. Origin of gabbro pegmatite in the Smartville intrusive complexe, northern Sierra Nevada, California. American Mineralogist 71, 1085-1099.

Bottinga, Y., Weill, F., 1970. Densities of liquid silicate systems calculated from partial molar volumes of oxide components. American Journal of Science 269, 169-182.

Bow, C., Wolfgram, D., Turner, A., Barnes, S., Evans, J., Zdepski, M., Boudreau, A., 1982. Investigations of the Howland reef of the Stillwater Complex, Minneapolis adit area : stratigraphy, structure, and mineralization. Economic Geology 77, 1481-1492.

Bremond d'Ars, J. de, 1990. Estimation des propriétés rhéologiques des magmas par l'étude des instabilités gravitaires. Pétrologie du complexe plutonique de Guernesey. Mémoires

et Documents du Centre Armoricain d'Etude Structurale des Socles (Thesis), Rennes 35, 370 p.

Bremond d'Ars, J. de, Davy, P., 1991. Gravity instabilities in magma chambers – rheological modeling. Earth and Planetary Science Letters 105, 319-329.

Bremond d'Ars, J. de, Martin, H., Auvray, B., Lécuyer, C., 1992. Petrology of a magma chamber: the plutonic complex of Guernsey (Channel Islands, UK). Journal of the Geological Society of London 149, 701-708.

Briden, J.C., Clark, A., Fairhead, J.D., 1982. Gravity and magnetic studies in the Channel Islands. Journal of the Geological Society of London 139, 35-48.

Cabanis, B., Lecolle, M., 1989. Le diagramme La/10-Y/15-Nb/8: un outil pour la discrimination des séries volcaniques et la mise en évidence des processus de mélange et/ou de contamination crustale. Comptes Rendus de l'Académie des Sciences de Paris 309, série II, 2023-2029.

Capdevila, R., 2010. Les granites varisques du Massif armoricain. Bulletin de la Société Géologique et Minéralogique de Bretagne (D) 7, 1-52.

Caroff, 1995. Open system crystallization and mixing in two-layer magma chambers. Lithos 36, 85-102.

Caroff, M., Ambrics, C., Maury, R.C., Cotten, J., 1997. From alkali basalt to phonolite in handsize samples: vapor-differentiation effects in the Bouzentès lava flow (Cantal, France). Journal of Volcanology and Geothermal Research 79, 47-61.

Caroff, M., Guillou, H., Lamiaux, M., Maury, R.C., Guille, G., Cotten, J., 1999. Assimilation of ocean crust by hawaiitic and mugearitic magmas: an example from Eiao (Marquesas). Lithos 46, 235-258.

Cawthorn, R.G., Boerst, K., 2006. Origin of the pegmatitic pyroxenite in the Merensky Unit, Bushveld Complex, South Africa. Journal of Petrology 47, 1509-1530.

Chantraine, J., Chauris, L., Cabanis, B., Chauris, M.-M., Larsonneur, C., Herrouin, Y., Rabu, D., Lulzac, Y., Bos, P., 1986. Notice explicative, carte géol. France (1/50 000), feuille Plestin-Les-Grèves (202). Orléans, BRGM, 84 p. Geological map by J. Chantraine *et al.* (1985).

Chapman, M., Rhodes, J.M., 1992. Composite layering in the Isle au Haut Maine igneous complex, Maine: Evidence for periodic invasion of a mafic magma into an evolving magma reservoir. Journal of Volcanology and Geothermal Research 51, 41-60.

Coint, N., Caroff, M., Hallot, E., Peucat, J.J., 2009. The gabbro-diorite layered intrusions of Saint-Jean-du-Doigt (France) and Beaucette (Guernsey, Channel Island), Armorican Massif: an emplacement model. Geological Society of America Abstracts with Programs 41 (2), 30.

Coint, N., Hamelin, C., Caroff, M., 2008. Le complexe gabbro-dioritique lité de Saint-Jean-du-Doigt, Massif armoricain: un exemple de réservoir magmatique de type MASLI. Bulletin de la Société Géologique et Minéralogique de Bretagne (D) 5, 1-29.

Collins, W.J., Wiebe, R.A., Healy, B., Richards, S.W., 2006. Replenishment, crystal accumulation and floor aggradation in the megacrystic Kameruka suite, Australia. Journal of Petrology 47, 2073-2104.

Cordier, C., Caroff, M., Juteau, T., Fleutelot, C., Hémond, C., Drouin, M., Cotten, J., Bollinger, C., 2007. Bulk-rock geochemistry and plagioclase zoning in lavas exposed along the northern flank of the Western Blanco Depression (Northeast Pacific): Insight into open-system magma chamber processes. Lithos 99, 289-311.

Cotten, J., Le Dez, A., Bau, M., Caroff, M., Maury, R., Dulski, P., Fourcade, S., Bohn, M., Brousse, R., 1995. Origin of anomalous rare-earth element and yttrium enrichments in subaerial exposed basalts: Evidence from French Polynesia. Chemical Geology 119, 115-138.

De Paolo, D.J., 1988. Neodymium isotope geochemistry, an introduction. Mineral and rocks, 20. Springer Verlag, Berlin, Heidelberg.

D'Lemos, R.S., 1996. Mixing between granitic and dioritic crystal mushes, Guernsey, Channel Islands, UK. Lithos 38, 233-257.

Elwell, R.W.D., Skelhorn, R.R., Drysdall, A.R., 1960. Inclined granitic pipes in the diorites of Guernsey. Geological Magazine 97, 89-105.

Elwell, R.W.D., Skelhorn, R.R., Drysdall, A.R., 1962. Net veining in the diorite of north east Guernsey, Channel Islands. Journal of Geology 70, 215-226.

Fernandez, A.N., Barbarin, B., 1991. Relative rheology of coeval mafic and felsic magmas : Nature of resulting interaction processes and shape and mineral fabrics of mafic microgranular enclaves. In: Didier, J., Barbarin, B. (Eds), Enclaves and granite petrology. Elsevier, Amsterdam, p. 263-275.

Fernandez, A.N., Gasquet, D.R., 1994. Relative rheological evolution of chemically contrasted coeval magmas: example of the Tichka plutonic complex (Morocco). Contributions to Mineralogy and Petrology 116, 316-326.

Franceschelli, M., Puxeddu, M., Cruciani, G., Dini, A., Loi, M., 2005. Layered amphibolite sequence in NE Sardinia, Italy : remnant of a pre-Variscan mafic silicic layered intrusion ? Contributions to Mineralogy and Petrology 149, 164-180.

Graviou, P, Auvray, B., 1985. Caractérisation pétrographique et géochimique des granitoïdes cadomiens du domaine nord-armoricain: implications géodynamiques. Comptes Rendus de l'Académie des Sciences de Paris 301, 315-318.

Hallot, E., Davy P., Bremond d'Ars J. de, Auvray, B., Martin H., Van Damme H., 1996. Non-newtonian effects during injection in partially crystallized magmas. Journal of Volcanology and Geothermal Research 71, 31-44.

Hellström, F.A., Johansson, A., Larson, S.A., 2004. Age and emplacement of late Sveconorwegian monzogabbroic dykes, SW Sweden. Precambrian Research 128, 39-55.

Johnson, M.C., Rutherford, M.J., 1989. Experimental calibration of the aluminium-in-hornblende geobarometer with application to Long Valley caldera (California) volcanic rocks. Geology 17, 837-841.

La Roche, H. de, Leterrier, J., Grandeclaude, P., Marchal, M., 1980. A classification of volcanic and plutonic rocks using R1R2-diagrams and major-element analyses – its relationships with current nomenclature. Chemical Geology 29, 183-210.

López-Moro, F.J., López-Plaza, M., 2004. Monzonitic series from the Variscan Tormes Dome (Central Iberian Zone): petrogenetic evolution from monzogabbro to granite magmas. Lithos 72, 19-44.

McBirney, A.R., Noyes, R.M., 1979. Crystallization and layering of the Skaergaard intrusion. Journal of Petrology 20, 487-554.

McEllen, A.T., 2006. Pegmatites of the Mount Sheridan gabbro, Wichita Mountains, Oklahoma. Geological Society of America Abstracts with Programs 38 (1), 5.

Momme, P., Wilson, J.R., 2002. The Kraemer Island macrodyke, East Greenland: solidification of a flood basalt conduit. Geological Magazine 139, 171-190.

Paterson, S.R., 2009. Magmatic tubes, pipes, troughs, diapirs, and plumes: Late-stage convective instabilities resulting in compositional diversity and permeable networks in crystal-rich magmas of the Tuolumne batholith, Sierra Nevada, California. Geophere 5, 496-527.

Petford, N., 2009. Which effective viscosity? Mineralogical Magazine 73, 167-191.

Peucat, J.J., Ménot, R.-P., Monnier, O., Fanning, C.M., 1999. The Terre Adélie basement in the East-Antarctica shield: geological and isotopic evidence for a major 1.7 Ga thermal

event; comparison with the Gawler Craton in South Australia. Precambrian Research 94, 205-224.

Philpotts, A.R., Carroll, M., Hill, J.M., 1996. Crystal-mush compaction and the origin of pegmatitic segregation sheets in a thick flood-basalt flow in the Mesozoic Hartford Basin, Connecticut. Journal of Petrology 37, 811-836.

Pons, J., Barbey, P., Nachit, H., Burg, J.-P., 2006. Development of igneous layering during growth of pluton: The Tarçouate Laccolith (Morocco). Tectonophysics 413, 271-286.

Roach, R.A., 1971. The layered structure of the St Peter Port Gabbro, Guernsey, Channel Isles (abstract). Journal of the Geological Society of London 127, 295.

Samson, S.D., D'Lemos, R.S., 1998. U-Pb geochronology and Sm-Nd isotopic composition of Proterozoic gneisses, Channel Islands, UK. Journal of the Geological Society of London 155, 609-618.

Samson, S.D., D'Lemos, R.S., 1999. A precise late Neoproterozoic U-Pb zircon age for the syntectonic Perelle quartz diorite, Guernsey, Channel Islands, UK. Journal of the Geological Society of London 156, 47-54.

Schmidt, M.W., 1992. Amphibole composition in tonalite as a fonction of pressure: an experimental calibration of the Al-in-hornblende barometer. Contributions to Mineralogy and Petrology 110, 304-310.

Sparks, R.S.J., Huppert, H.E., 1984. Density changes during fractional crystallization of basaltic magmas: fluid dynamic implications. Contributions to Mineralogy and Petrology 85, 300-309.

Sparks, R.S.J., Huppert, H.E., Koyaguchi, T., Halloworth, M.A., 1993. Origin of modal and rhythmic igneous layering by sedimentation in a convecting magma chamber. Nature 361, 246-249.

Sparks, R.S.J., Marshall, L.A., 1986. Thermal and mechanical constraints on mixing between mafic and silicic magmas. Journal of Volcanology and Geothermal Research 29, 99-124.

Sparks, R.S.J., Meyer, P., Sigurdsson, H., 1980. Density variation amongst Mid-Ocean Ridge Basalts: implication for magma mixing and the scarcity of primitive lavas. Earth and Planetary Science Letters 46, 419-430.

Stewart, B.W., De Paolo, D.J., 1992. Diffusive isotopic contamination of mafic magma by coexisting silicic liquid in the Muskox intrusion. Science 255, 708-711.

Sun, S.S., McDonough, W.F., 1989. Chemical and isotopic systematics of oceanic basalts: implication for mantle composition and processes. In: Saunder, A.D., Norry, M.J. (Eds), Geological Society Special Publication. Magmatism in the Ocean Basins, vol. 42. Blackwell, London, p. 313-345.

Topley, C.G., Brown, M., D'Lemos, R.S., Power, G.M., Roach, R.A., 1990. The northern igneous complex of Guernsey, Channel Islands. R.S. D'Lemos, R.A. Strachan and C.G. Topley (Editors), The Cadomian Orogeny. Geological Society Special Publication 51, 245-259.

Topley, C.G., Brown, M., Power, G.M., 1982. Interpretation of field relationships of diorites and associated rocks with particular reference to northwest Guernsey, Channel Islands. Geological Journal 17, 323-343.

Waight, T.E., Wiebe, R.A., Krogstad, E.J., 2007. Isotopic evidence for multiple contributions to felsic magma chambers: Gouldsboro Granite, Coastal Maine. Lithos 93, 234-247.

Wiebe, R.A., 1974. Coexisting intermediate and basic magmas, Ingonish, Cape Breton Island. Journal of Geology 82, 74-87.

Wiebe, R.A., 1993a. Basaltic injections into floored silicic magma chambers. Eos, Transactions, American Geophysical Union 74, 1, 3.

Wiebe, R.A., 1993b. The Pleasant Bay layered gabbro-diorite, Coastal Maine: Ponding and crystallization of basaltic injections into a silicic magma chamber. Journal of Petrology 34, 461-489.

Wiebe, R.A., 1994. Silicic magma chambers as traps for basaltic magmas: The Cadillac Mountain intrusive complex, Mount Desert Island, Maine. Journal of Geology 102, 423-437.

Wiebe, R.A., 1996. Mafic-silicic layered intrusions: the role of basaltic injections on magmatic processes and the evolution of silicic magma chambers. Transactions of the Royal Society of Edinburgh: Earth Sciences 87, 233-242.

Wiebe, R.A., Collins, W.J., 1998. Depositional features and stratigraphic sections in granitic plutons: implications for the emplacement and crystallization of granitic magma. Journal of Structural Geology 20, 1273-1289.

Wiebe, R.A., Frey, H., Hawkins, D.P., 2001. Basaltic pillow mounds in the Vinalhaven intrusion, Maine. Journal of Volcanology and Geothermal Research 107, 171-184.

Wiebe, R.A., Smith, D., Sturm, M., King, E.M., Seckler, M.S., 1997. Enclaves in the Cadillac Mountain Granite (Coastal Maine): Samples of hybrid magma from the base of the chamber. Journal of Petrology 38, 393-423.

Wiebe, R.A., Wark, D.A., Hawkins, D.P., 2007. Insights from quartz cathodoluminescence zoning into crystallization of the Vinalhaven granite, coastal Maine. Contributions to Mineralogy and Petrology 154, 439-453.

Figure captions

Fig. 1. Geological sketch maps, location of detailed maps (including those of Fig. 2) and of samples. a. North Armorican domains. b. Saint-Jean-du-Doigt intrusive complex (SJIC), from

Chantraine et al. (1986). Ages from Barboni et al. (2010). c. North-Guernsey intrusive complex (NGIC), contours and ages from Bremond d'Ars et al. (1992) and Samson and D'Lemos (1998, 1999).

Fig. 2. Geological sketch map of noteworthy outcrops and sample location. a. Poul Rodou, b. Roc'h Louet, and c. Primel from the SJIC (this work). d. The Beaucette Battery, and e. The Beaucette pass from the NGIC (this work and Bremond d'Ars et al., 1992).

Fig. 3. Photographs of sheets and diapirs in the SJIC sampled sections. a. Section SJ34 and sample position. Hammer for scale. b. Section SJ43 and sample position. Hammer for scale. c. A dioritic sheet with feeding roots, under a xenolith. d. A concave-down diapir within the gabbro, just below a not visible dioritic sheet.

Fig. 4. Mixing, mingling, magmatic brecciation and pegmatoid in the SJIC (Saint-Jean's bay). a. Gabbroic pillow-like enclave with a chilled margin, enclosed in a heterogeneous monzogabbro (mingling). b. Ribbon rocks in the process of hybridization (mingling/mixing). Hammer for scale. c. Jigsaw-type breccias with polyhedral mafic enclaves enclosed in a texturally homogeneous (intergranular) monzonite forming a vein network. A few blocky clasts present mixing/mingling evidence (not visible). d. Mafic cumulate-aplite-pegmatoid association. Sample PM2 (three analyses in Table 1).

Fig. 5. Sheets and diapirs in the NGIC. a. Photograph of section GS10 and sample position. Hammer for scale. b. Detail: gabbroic sheet and inclined pipes. Pencil for scale. c. Photograph of section GS13 and sample position. d. Sketch of the dioritic veins. e. Sketch of the inclined pipes. f. Cross-section through a zoned pipe, with a core (dark gray) less

909 differentiated than the rim (light gray), a pegmatitic upper part (white), and altered overlying
910 host rock. d, e and f from Elwell et al. (1960).
911
912 Fig. 6. Cumulates and pegmatoids from the NGIC (Spur Point, Saint Peter Port gabbro). a.
913 Mottled orthocumulate showing layers of poikilitic amphibole crystal flecks. Pencil for scale.
914 b. Photomicrograph (crossed nicols) of the Spur Point mottled orthocumulate (sample GS1a,
915 fleck-free white layer). Cumulus minerals are calcic plagioclase (Pl), hornblende (Hb) and
916 clinopyroxene (Cpx). By decreasing abundance, intercumulus phases are plagioclase,
917 clinopyroxene, orthopyroxene, Fe-Ti oxides, and apatite. c. Mafic cumulate-pegmatoid
918 association.
919
920 Fig. 7. NGIC plagioclase compositions. a. Anorthite content in plagioclases of samples GS1a
921 (26 analyses), GS7d, e, l (21 analyses), and GS13a (16 analyses). b. Anorthite profile through
922 a plagioclase from GS13a.
923
924 Fig. 8. Chemical sections in the SJIC. MgO, TiO_2 and Al_2O_3 concentrations through sections
925 SJ34 and SJ43 (located in Fig. 2a and shown in Fig. 3a and b). Microtextural sketches, shown
926 for samples SJ34a, d2, and e, evidence the lack of chilled margins (white: plagioclase; grey:
927 amphibole and altered olivine; black: Fe-Ti oxides).
928
929 Fig. 9. Chemical sections in the NGIC. MgO, TiO_2 and Al_2O_3 contents through sections
930 GS10-13 and GS7 (located in Fig. 2d and e).
931
932 Fig. 10. Magmatic affinities of the mafic rocks from the SJIC and NGIC. Position of the
933 gabbroic samples in the diagram La/10-Y/15-Nb/8 (Cabanis and Lecolle, 1989).

934

935 Fig. 11. Chondrite C1-normalized rare earth elements (REE) patterns of representative SJIC
936 and NGIC samples. Normalization values from Sun and McDonough (1989). a. Sheet-diapir
937 pairs SJ34 and SJ43, together with the corresponding gabbroic field (SJIC). b. Selected SJIC
938 samples. c. Macrorhythms, sheets and a pipe from the NGIC. d. Granite, sheet and cumulate
939 from the NGIC.

940

941 Fig. 12. Models of replenishment and crystallization. Time proceeds along the "*t*-box" line.
942 a. b. c. Model for Poul Rodou in the SJIC. A gabbroic (θ) reservoir crystallizes from below:
943 crystal settling is negligible so that the resulting gabbro is almost homogeneous. A dioritic
944 magma (δ) with about χ=30% phenocrysts enters the crystallizing gabbro. First buoyant at the
945 base, while rising it crosses levels of neutral buoyancy (assuming negligible crystal
946 resorption) where it spreads to form sheets from which diapirs are then extracted. ρ is density
947 at given temperature (calculated from Bottinga and Weill, 1970) and crystal content (χ for δ;
948 grey scale to the right for θ; see text). Insets are detailed zones of a and b.
949 d. e. f. g. h. i. Model for Beaucette in the NGIC. Mafic recharges (d, g) and crystal settling,
950 first of mafic minerals alone (e), second of mafic crystals and plagioclase (f) account for the
951 layering and the heterogeneities of the gabbros. Then late dioritic recharges (h) and
952 subsequent evolution (i, see text) explain most of the observed features.

953

954 Fig. 13. A comprehensive model for the SJIC reservoir. The straight line locates the observed
955 Poul Rodou/Saint-Jean's bay/Primel coastal cross-section. See text for explanations.

Table 1. Chemical data (wt% oxide, ppm element) on whole rock samples from Saint-Jean-du-Doigt and North-Guernsey.

Location		R. Louet	P. Rodou	Primel	Primel	St-J. W	St-J W	St-J E	P. Rodou	P. Rodou	P. Rodou	P. Rodou	P.Rodou	P. Rodou	P. Rodou
Sample		SJ32	SJ44b	SJ16	SJ14	SJ37	SJ9	SJ17	SJ22	SJ34a	SJ34c	SJ34b1	SJ43a	SJ43c	SJ43d
Texture		Cum.	Gr./Cum	Peg.	Dol.	Gr.	Gr.	Gr.	Gr.	Gr.	Gr.	Gr./Cum.	Gr.	Gr.	Gr./Peg.
Emplacement		Cum.	Intrusion	Intrusion	Dyke	Fl. cl	Fl. cl.	Ang. Cl	Intrusion	Intrusion	Sheet	Diapir	Intrusion	Sheet*	Diapir
Type		Melagab.	Melagab.	Gabbro	Gabbro	Mzgab.	Monz.	Q-Monz.	Granite	Gabbro	Diorite	Diorite	Gabbro	Q-Monz.	Q-Monz.
SiO_2	(wt.%)	44.20	47.10	49.20	50.20	53.25	58.60	71.60	76.75	49.70	60.80	58.80	50.00	72.20	74.00
TiO_2		0.80	0.64	1.92	2.22	2.42	1.37	0.35	0.13	1.81	1.24	0.65	1.79	0.33	0.13
Al_2O_3		14.32	14.22	15.40	14.53	14.80	17.75	15.70	12.05	15.00	15.55	16.90	15.42	14.05	10.62
$Fe_2O_3^t$		12.80	9.40	9.80	9.96	11.58	7.00	0.86	1.62	10.90	5.58	5.80	11.25	1.98	4.32
MnO		0.21	0.15	0.14	0.19	0.20	0.10	0.01	0.02	0.19	0.10	0.09	0.18	0.03	0.03
MgO		13.00	13.90	6.85	6.92	3.69	1.92	0.52	0.10	6.80	2.47	1.18	7.23	0.78	0.19
CaO		10.30	8.50	11.47	12.15	7.20	5.00	2.60	0.24	9.40	8.40	14.60	7.38	2.14	8.70
Na_2O		0.88	1.52	2.85	2.69	3.67	5.55	7.00	3.38	2.86	4.50	0.23	2.48	6.85	0.29
K_2O		0.26	0.85	0.48	0.22	1.46	1.49	0.45	4.70	1.13	0.37	0.23	2.30	0.36	0.24
P_2O_5		0.03	0.14	0.14	0.30	0.72	0.32	0.05	0.02	0.23	0.26	0.19	0.25	0.05	0.02
L.O.I.		3.48	3.41	1.27	0.61	0.64	0.81	0.60	0.56	1.83	1.02	1.60	2.08	0.58	1.02
Total		100.07	99.83	99.52	99.99	99.63	99.91	99.74	99.57	99.85	100.29	100.27	100.36	99.35	99.56
Rb	(ppm)	7.5	27.4	17.3	6.4	42.4	42.5	13.5	185	37.5	9.4	7.9	111	8.6	15.5
Sr		142	253	239	145	218	235	243	23	233	322	695	121	84	445
Ba		50	123	91	19	405	405	116	324	286	90	49	330	35	32
Sc		29.0	29.5	47	45	28.0	8.7	4.0	2.5	40	17	6.5	38	5.2	1.2
V		143	210	405	347	265	145	29	4	290	147	90	281	52	32
Cr		216	955	38	103	35	9	10	3.5	255	25	13	225	11	5
Co		70	57	38	47	25	15	3	2	39	11	5	41	5	2
Ni		213	380	44	55	19	9	7	2	70	17	12	72	7	4
Y		9.6	5.6	23.5	38.0	65	38.8	23.5	54	32.5	47.0	33.0	30.5	21.8	9.3
Nb		2.8	2.5	7.9	14.3	37.5	25.0	17.5	30.0	16.0	30.5	21.5	14.0	15.4	5.2
La		2.5	7.1	6.4	10.8	35.0	29.5	12.8	30.0	11.0	20.5	27.0	11.0	10.0	24.5
Ce		5.3	16.0	14.5	25.0	80	60	25.5	86	25.0	45	56	24.0	16.5	38.0
Nd		3.4	10.0	11.2	17.8	45.0	30.5	12.2	28.5	17.0	26.6	27.0	16.0	8.0	11.0
Sm		1.35	2.70	2.95	5.1	10.4	6.4	2.70	6.6	4.7	6.4	5.5	4.5	2.25	1.75
Eu		0.61	0.84	1.10	1.78	2.67	2.62	0.88	0.60	1.56	1.68	1.89	1.44	1.08	1.11
Gd		1.2	2.7	4.1	6.5	11.0	7.2	3.1	6.9	5.7	7.6	5.8	5.2	2.9	2.1
Dy		1.55	2.45	4.1	6.5	10.9	6.4	3.60	8.2	5.5	7.8	5.4	5.4	3.15	1.4
Er		0.9	1.5	2.2	3.7	6.1	3.7	2.3	5.5	3.1	4.6	3.3	3.1	2.2	1.0
Yb		0.90	1.48	2.10	3.42	5.60	3.62	2.38	6.52	2.92	4.46	3.36	2.90	2.20	1.01
Th		0.30	1.15	1.25	0.55	3.50	5.05	14.7	17.3	1.40	6.15	12.3	1.20	13.7	4.50

ICP-AES analyses (analyst: Jo Cotten, Brest). Cum.: Cumulat; Gr.: Granular (broad sense); Peg.: pegmatitic; Dol.: Doleritic; Apl.: Aplitic; Fl. cl.: Fluidal clast; Ang. cl.: Angular clast; Sheet*: upper part of a sheet; L.O.I.: Loss on ignition.

Table 1 (continuation).

Location		Primel	Primel	Primel	Spur	Cobo	Beaucette	Beaucette	Beaucette	Beaucette	Beaucette	Beaucette	Beaucette	Beaucette
Sample		PM2a	PM2b	PM2c	GS1a	GS8	GS10d	GS10f	GS13a	GS10c	GS7a	GS7e	GS7j	GS7c
Texture		Peg.	Apl.	Cum.	Cum.	Gr.	Gr./Cum.	Gr./Cum.	Gr.	Gr.	Gr./Cum.	Gr. /Cum.	Gr./Cum.	Gr.
Emplacement		Intrusion	Intrusion	Cum.	Cum.	Intrusion	Macrorh.	Macrorh.	Sheet	Diapir	Macrorh	Macrorh	Macrorh	Sheet
Type		Gabbro	Gabbro	Gabbro	Gabbro	Granite	Melagab.	Gabbro	Gabbro	Mzdior.	Melagab.	Gabbro	Gabbro	Diorite
SiO_2	(wt.%)	52.60	48.40	49.00	45.30	76.00	47.70	49.70	48.50	61.80	49.30	53.50	51.90	66.20
TiO_2		0.59	0.57	0.39	1.16	0.10	0.57	0.82	1.09	0.06	0.63	0.82	0.74	0.13
Al_2O_3		17.30	17.25	19.20	20.45	12.40	11.75	18.15	20.80	21.40	13.50	16.85	15.80	16.30
$Fe_2O_3^t$		5.16	7.67	5.70	9.55	1.48	10.45	8.93	9.75	1.35	9.00	8.60	8.15	1.60
MnO		0.09	0.11	0.09	0.13	0.05	0.17	0.15	0.14	0.03	0.14	0.14	0.12	0.02
MgO		6.50	8.85	7.34	5.56	0.24	14.35	6.09	3.60	1.14	12.30	5.23	7.35	1.08
CaO		12.45	12.15	14.10	14.00	0.55	9.20	10.40	9.75	5.32	9.60	8.18	9.40	7.10
Na_2O		3.40	2.21	2.17	1.75	3.61	1.20	2.88	3.40	5.89	2.08	3.21	3.00	5.20
K_2O		0.32	0.13	0.13	0.97	3.23	0.88	0.80	1.03	1.51	0.95	1.38	1.25	0.52
P_2O_5		0.10	0.04	0.03	0.21	0.04	0.09	0.14	0.27	0.05	0.08	0.14	0.12	0.17
L.O.I.		1.61	2.27	2.02	1.07	0.92	3.25	1.45	1.59	1.46	2.12	1.73	1.91	1.98
Total		100.12	99.65	100.17	100.15	98.62	99.61	99.51	99.92	100.01	99.70	99.78	99.74	100.30
Rb	(ppm)	11.5	3.3	3.7	27.2	124	26.0	20.0	29.5	42.0	28.0	40	35.0	13.2
Sr		277	217	266	872	113	172	420	590	867	340	430	340	280
Ba		54	25	22	300	656	298	226	481	351	370	310	190	88
Sc		44	44	44	38	3.3	37	34	26.0	3.9	40	31	44	5
V		184	202	154	317	8	205	253	246	12	210	242	232	28
Cr		179	232	240	72	4	855	195	18	8	1100	138	370	6
Co		25	35	25	32	2	59	31	24	5	50	30	37	7
Ni		50	72	70	24	2	242	42	9	12	265	35	86	8
Y		16.8	14.6	8.8	16.0	12.2	12.6	17.3	24.8	4.4	16.0	19	16.0	6.5
Nb		2.7	1.2	0.4	5.2	11.2	2.3	3.2	6.0	0.7	2.5	4.2	3.7	1.0
La		3.4	2.6	1.7	11.2	18.0	7.8	11.2	15.6	10.5	8.0	12.5	9.4	12.5
Ce		9.5	6.0	4.0	27.0	34.5	15.5	23.5	35	15	18.0	26.0	21.0	22.0
Nd		6.1	4.3	2.0	18.0	12.8	8.4	12.7	22.0	4.2	10.0	14.1	12.1	8.0
Sm		2.00	1.80	1.10	4.2	2.35	2.05	3.0	4.8	0.6	2.75	3.4	3.1	1.5
Eu		0.83	0.90	0.55	1.45	0.43	0.75	1.09	1.40	0.64	0.88	0.99	0.94	0.59
Gd		2.8	2.5	1.55	3.5	2.5	1.9	3.0	4.5	0.6	2.6	3.65	2.8	1.6
Dy		2.85	2.55	1.55	2.95	2.10	2.05	2.90	4.3	0.65	2.65	3.15	2.80	1.15
Er		1.6	1.5	0.8	1.5	1.3	1.3	1.7	2.4	0.5	1.6	1.9	1.6	0.6
Yb		1.50	1.31	0.78	1.30	1.49	1.18	1.67	2.28	0.56	1.62	1.83	1.58	0.57
Th		0.15	0.20	0.10	0.20	11.4	1.35	1.35	1.45	2.75	2.85	3.5	1.90	3.40

Table 2. Isotopic data on whole rock samples from Saint-Jean-du-Doigt and North-Guernsey.

Location	Type	Sample	Rb ppm	Sr ppm	$^{87}Rb/^{86}Sr$	$^{87}Sr/^{86}Sr$	$\pm 2\sigma m$ ($x10^{-6}$)	$(^{87}Sr/^{86}Sr)_i$	Sm ppm	Nd ppm	$^{147}Sm/^{144}Nd$	$^{143}Nd/^{144}Nd$	$\pm 2\ \sigma m$ ($x10^{-6}$)	ε_{Nd}
Saint-Jean-du-Doigt								*(t = 347 Ma)*						*(t = 347 Ma)*
Primel	Dolerite	SJ14	5.98	142	0.122	0.704655	11	0.7041	4.88	17.51	0.1684	0.512846	6	5.3
Primel	Peg.	SJ16	18.5	243	0.221	0.704947	9	0.7039	3.02	10.43	0.1750	0.512829	6	4.7
P. Rodou	Gabbro	SJ34a	38.0	230	0.477	0.707216	9	0.7049	4.22	15.88	0.1609	0.512860	4	5.9
P. Rodou	Diorite	SJ34c	8.71	296	0.085	0.707338	10	0.7069	6.28	25.38	0.1496	0.512668	7	2.6
St-J. W	Mzgab.	SJ37	42.1	208	0.586	0.707246	12	0.7043	10.04	43.62	0.1391	0.512633	7	2.4
St-J. W	Monz.	SJ9	42.3	226	0.541	0.707339	30	0.7047	6.36	30.04	0.1279	0.512632	5	2.9
St-J. E	Q-Monz.	SJ17	14.0	241	0.167	0.707263	10	0.7064	2.55	10.95	0.1407	0.512676	6	3.2
P. Rodou	Granite	SJ22	185	21.6	25.1	0.819524	15	0.6935	5.86	26.58	0.1334	0.512650	5	3.0
North-Guernsey (data from Brémond d'Ars et al., 1992)								*(t = 553 Ma)*						
Spur	Cum.	64A (GS1a)	18.1	891	0.059	0.70627	-	0.7058						
Beaucette	Melag.	27A (GS7a)	34.2	275	0.360	0.70842	-	0.7056						
Beaucette	Gabbro	26B (GS10f)	41.9	379	0.321	0.70836	-	0.7058						
Beaucette	G. sheet	27E (GS13a)	73.7	564	0.378	0.70867	-	0.7057						
Cobo	Granite	74-71 (GS8)	127	101	3.64	0.73417	-	0.7055						

See text for analytical methods and calculation of ε_{Nd}; index i for initial.

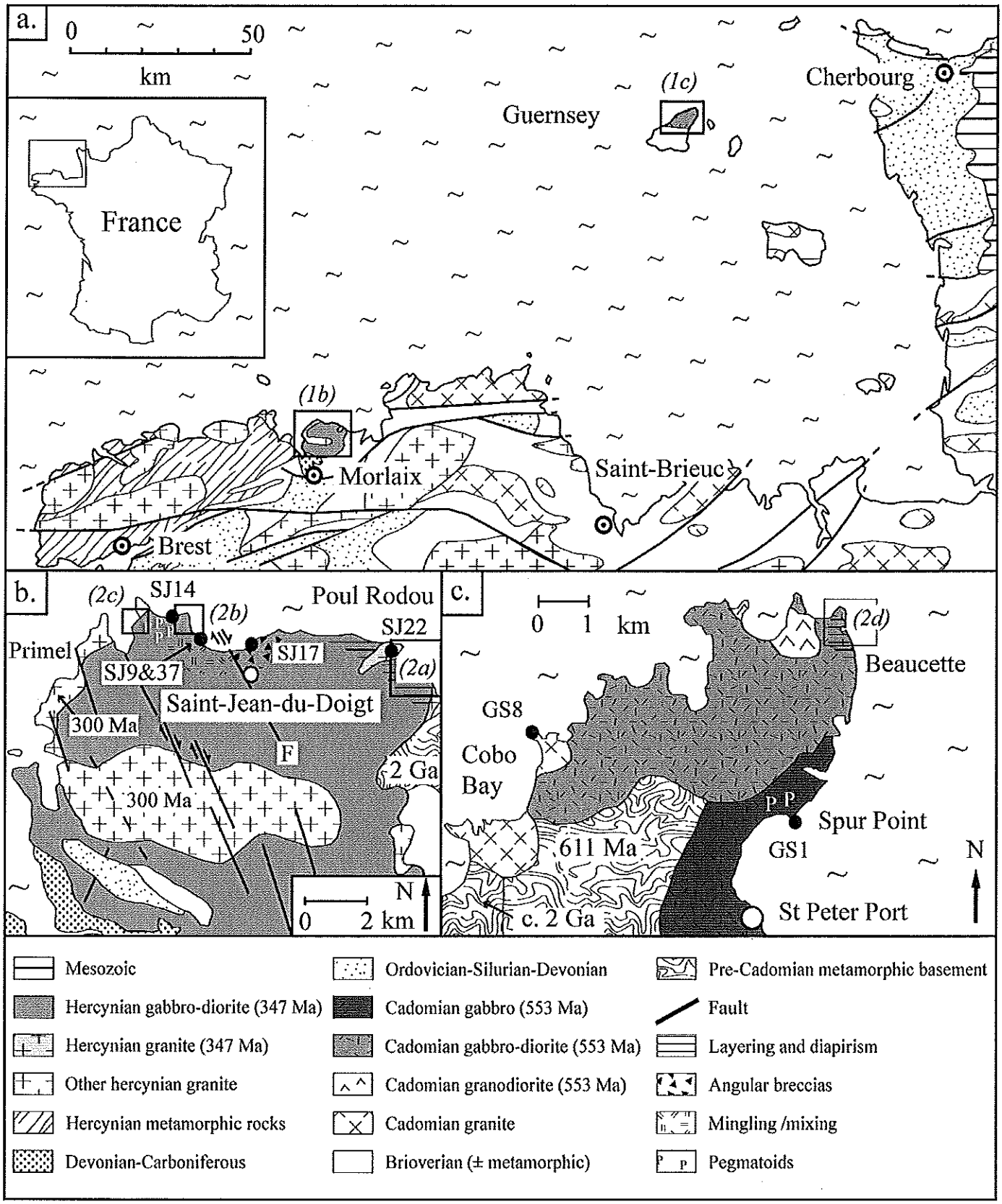
a.
0
50
km
France
Guernsey
(1c)
Cherbourg
(1b)
Morlaix
Saint-Brieuc
Brest
b.
(2c)
SJ14
(2b)
Poul Rodou
SJ22
Primel
SJ17
SJ9&37
(2a)
Saint-Jean-du-Doigt
300 Ma
F
2 Ga
300 Ma
N
0
2 km
c.
0
1
km
(2d)
Beaucette
GS8
Cobo
Bay
P P
Spur Point
611 Ma
GS1
N
c. 2 Ga
St Peter Port
Mesozoic
Hercynian gabbro-diorite (347 Ma)
Hercynian granite (347 Ma)
Other hercynian granite
Hercynian metamorphic rocks
Devonian-Carboniferous
Ordovician-Silurian-Devonian
Cadomian gabbro (553 Ma)
Cadomian gabbro-diorite (553 Ma)
Cadomian granodiorite (553 Ma)
Cadomian granite
Brioverian (± metamorphic)
Pre-Cadomian metamorphic basement
Fault
Layering and diapirism
Angular breccias
Mingling /mixing
Pegmatoids

Fig. 1

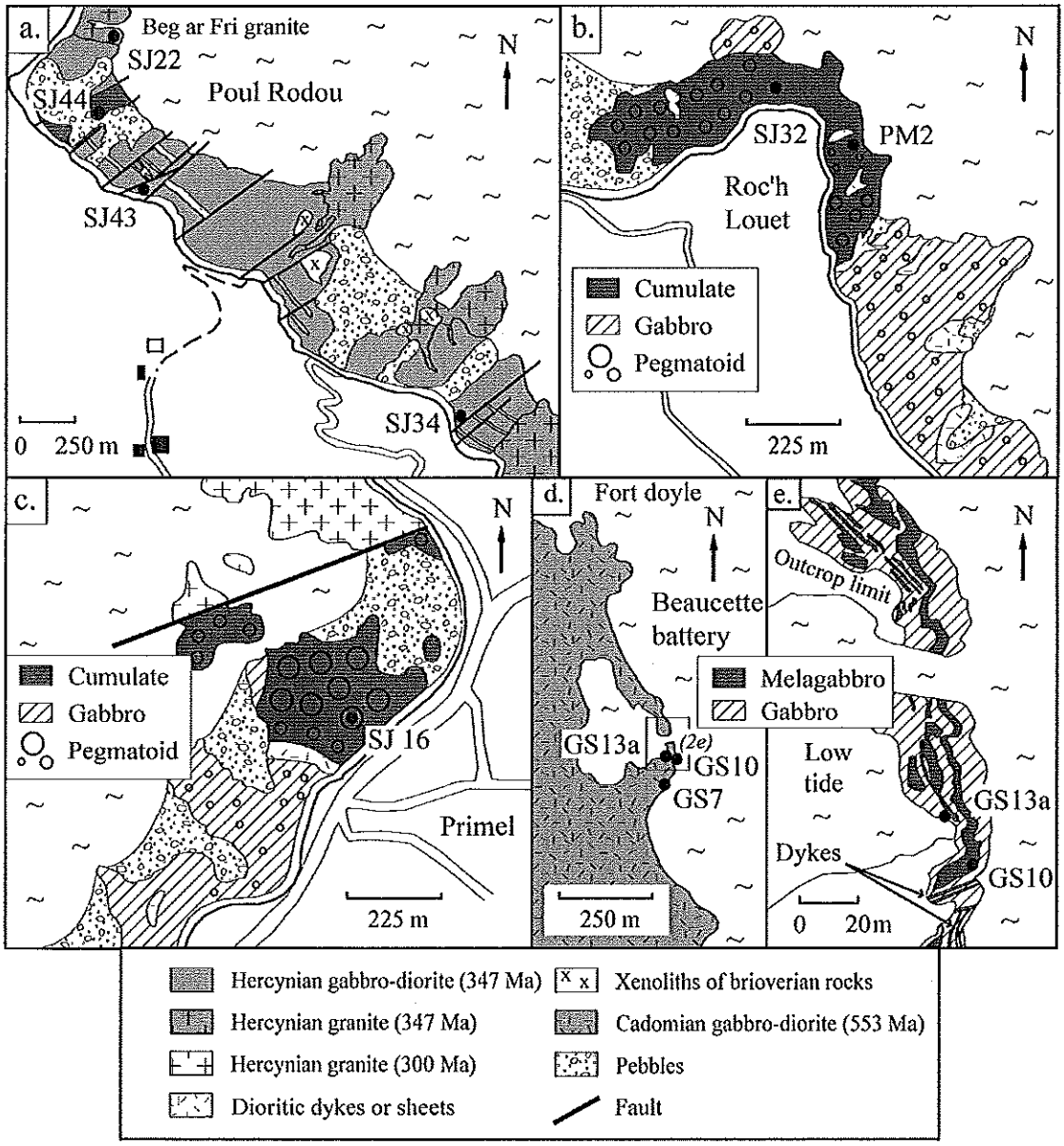
a.
Beg ar Fri granite
SJ22
SJ44
Poul Rodou
SJ43
SJ34
N
0 250 m
b.
SJ32
PM2
Roc'h
Louet
Cumulate
Gabbro
Pegmatoid
225 m
c.
Cumulate
Gabbro
Pegmatoid
SJ 16
Primel
225 m
d.
Fort doyle
Beaucette
battery
GS13a
(2e)
GS10
GS7
250 m
e.
Outcrop limit
Melagabbro
Gabbro
Low
tide
GS13a
GS10
Dykes
0 20m
Hercynian gabbro-diorite (347 Ma)
Hercynian granite (347 Ma)
Hercynian granite (300 Ma)
Dioritic dykes or sheets
Xenoliths of brioverian rocks
Cadomian gabbro-diorite (553 Ma)
Pebbles
Fault

Fig. 2

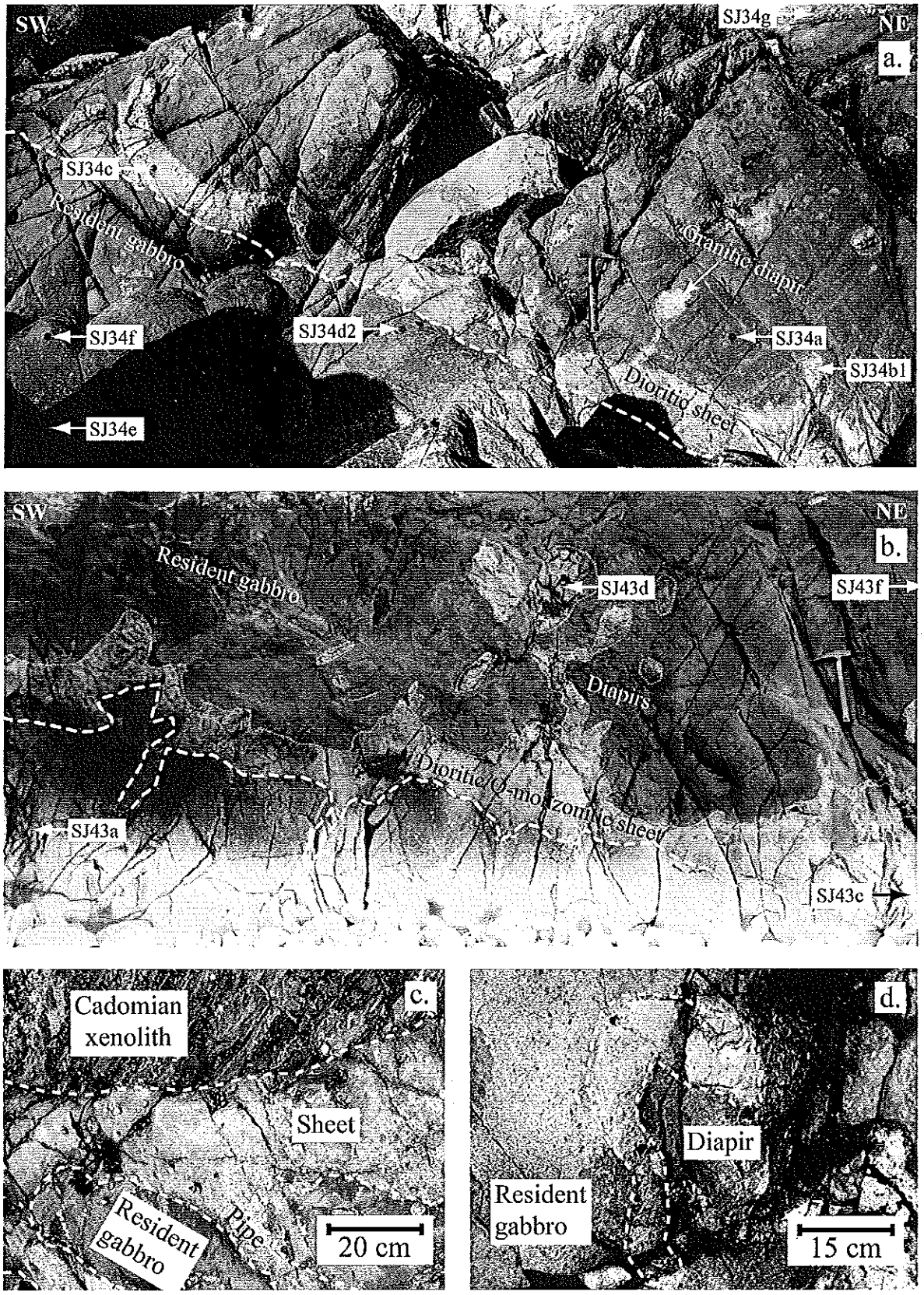
SW
SJ34g
NE
a.
SJ34c
Resident gabbro
Granitic diapir
SJ34f
SJ34d2
SJ34a
SJ34b1
Dioritic sheet
SJ34e
SW
NE
b.
Resident gabbro
SJ43d
SJ43f
Diapirs
Dioritic/Q-monzonitic sheet
SJ43a
SJ43c
c.
Cadomian xenolith
Sheet
Resident gabbro
Pipe
20 cm
d.
Diapir
Resident gabbro
15 cm

Fig. 3

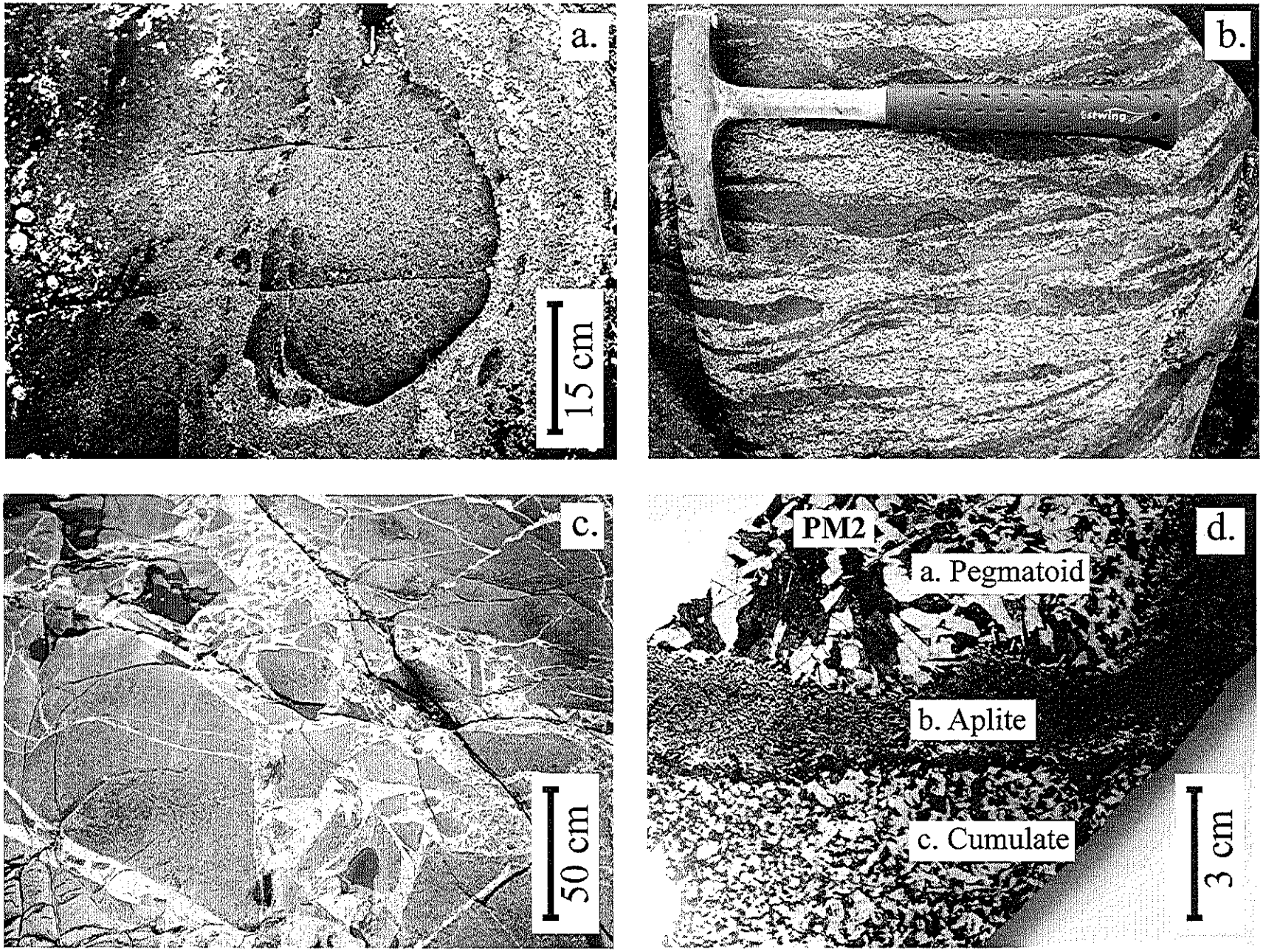

Fig. 4

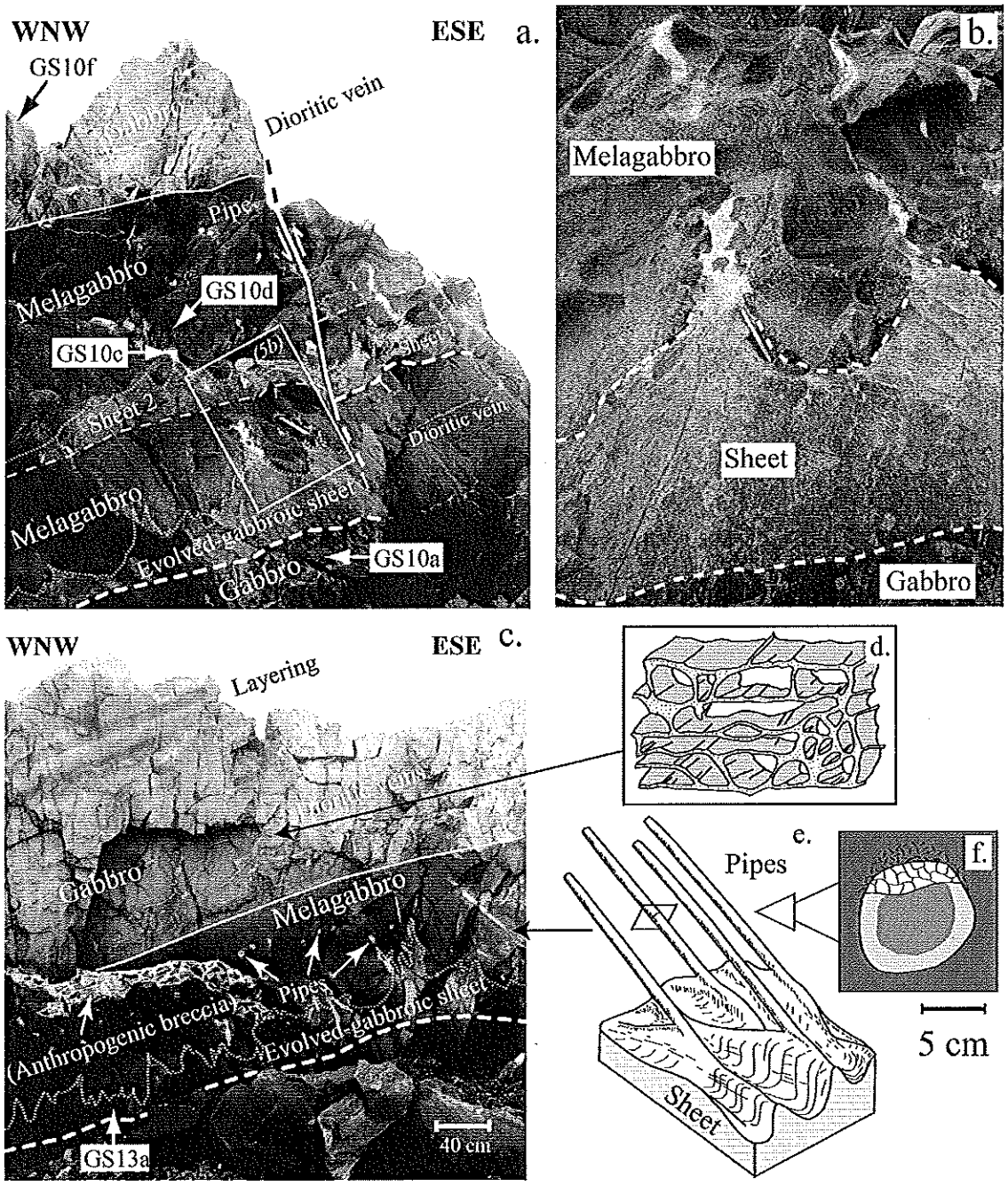
WNW
ESE
a.
GS10f
Dioritic vein
Pipe
Melagabbro
GS10d
GS10c
(5b)
Sheet 1
Sheet 2
Dioritic vein
Melagabbro
Evolved gabbroic sheet
GS10a
Gabbro
b.
Melagabbro
Sheet
Gabbro
WNW
ESE
c.
Layering
Gabbro
Melagabbro
Pipes
(Anthropogenic breccia)
Evolved gabbroic sheet
GS13a
40 cm
d.
e.
Pipes
f.
5 cm
Sheet

Fig. 5

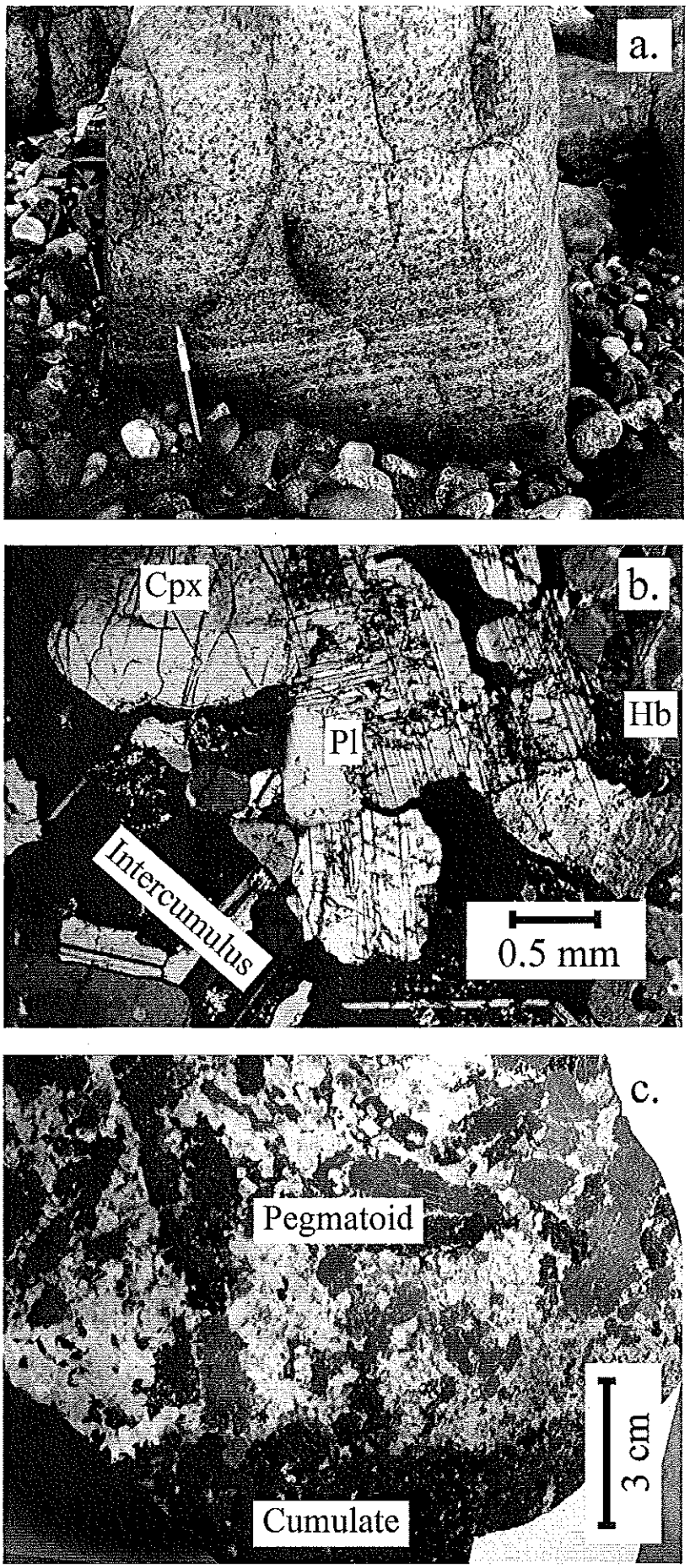

Fig. 6

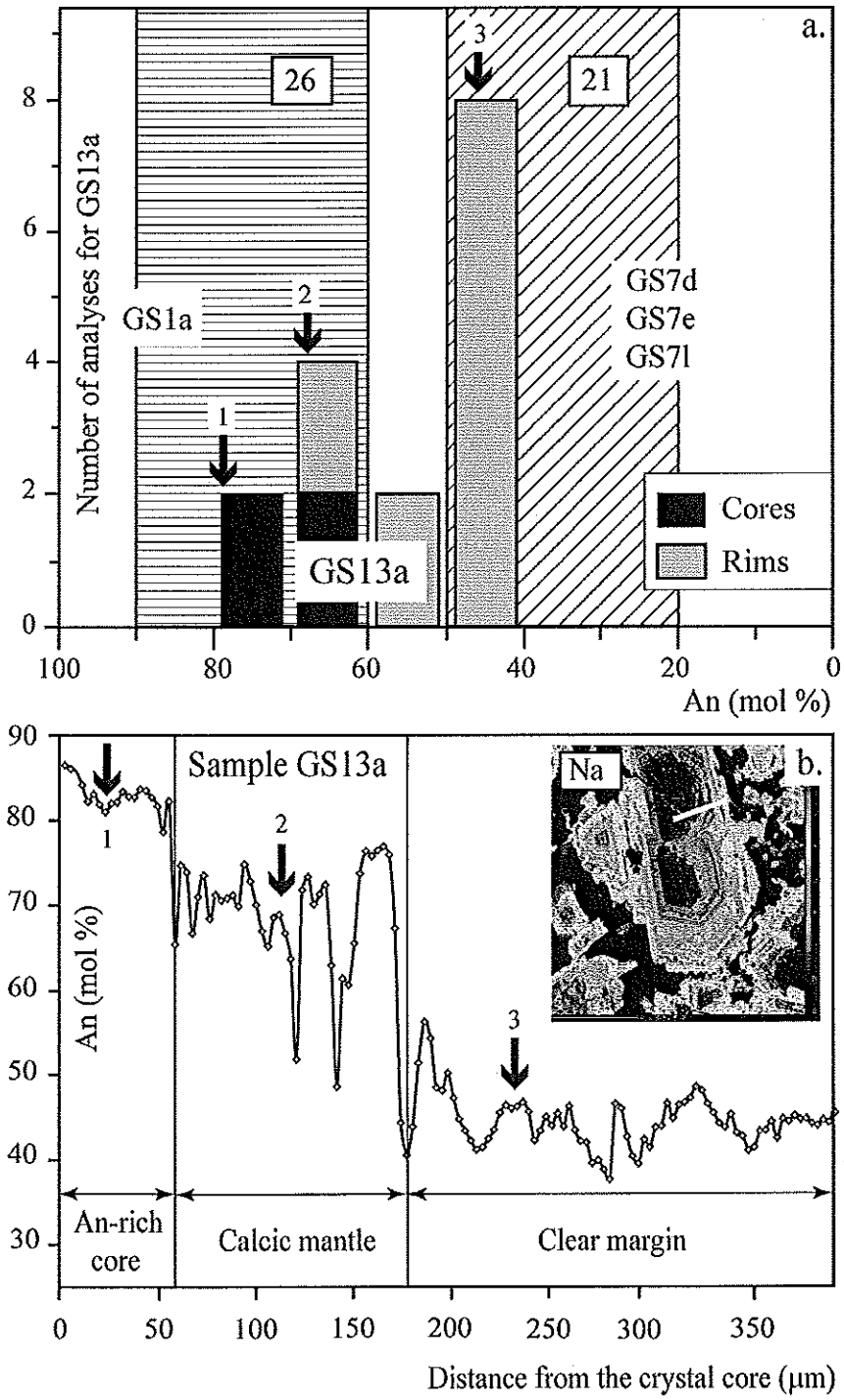
a.
Number of analyses for GS13a
26
21
GS1a
GS13a
GS7d
GS7e
GS7l
1
2
3
Cores
Rims
An (mol %)
b.
Sample GS13a
Na
An (mol %)
An-rich core
Calcic mantle
Clear margin
Distance from the crystal core (μm)

Fig. 7

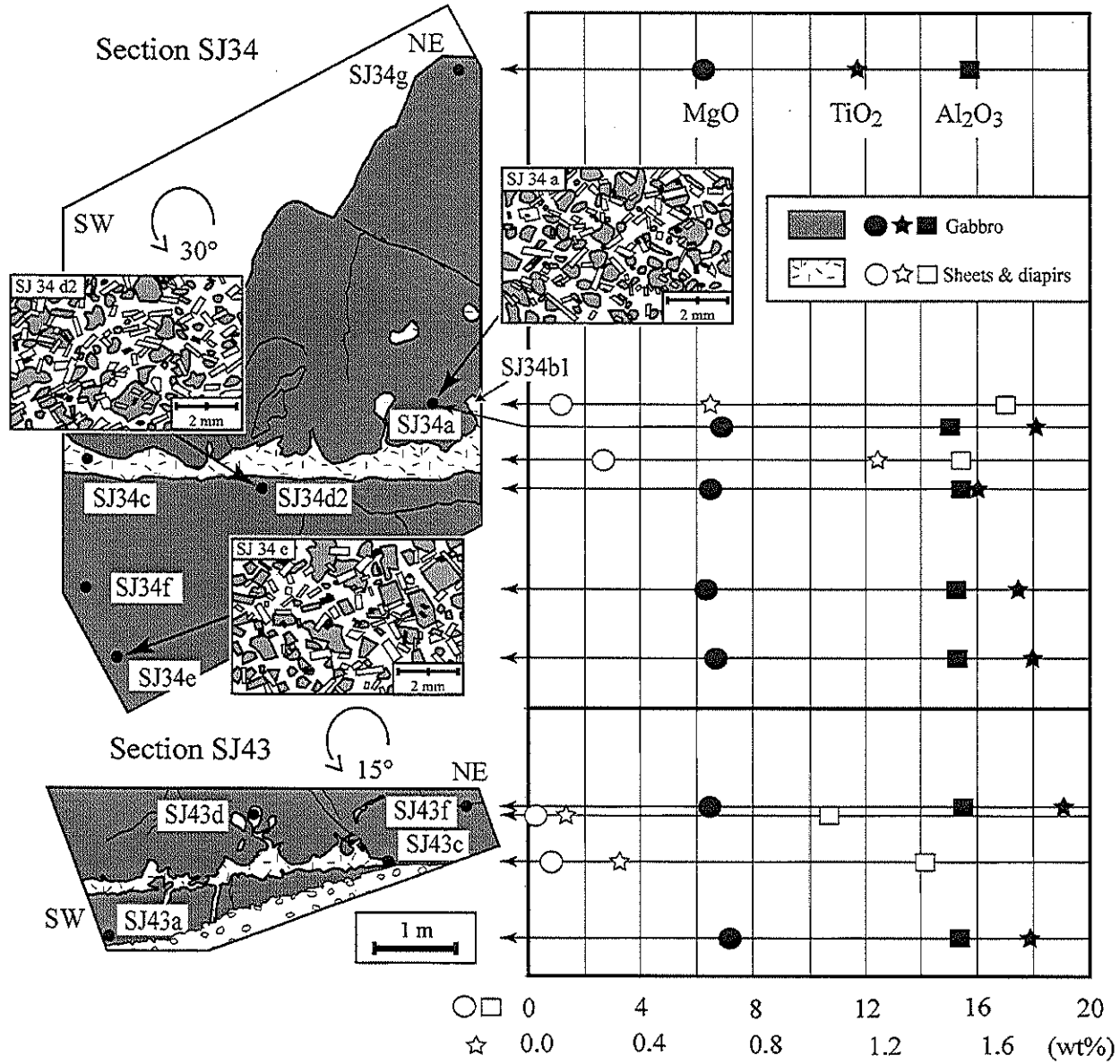
Section SJ34
NE
SJ34g
SW
30°
SJ 34 d2
2 mm
SJ 34 a
2 mm
SJ34b1
SJ34a
SJ34c
SJ34d2
SJ 34 e
2 mm
SJ34f
SJ34e
Section SJ43
15°
NE
SJ43d
SJ43f
SJ43c
SW
SJ43a
1 m
MgO
TiO2
Al2O3
Gabbro
Sheets & diapirs
0
4
8
12
16
20
0.0
0.4
0.8
1.2
1.6
(wt%)

Fig. 8

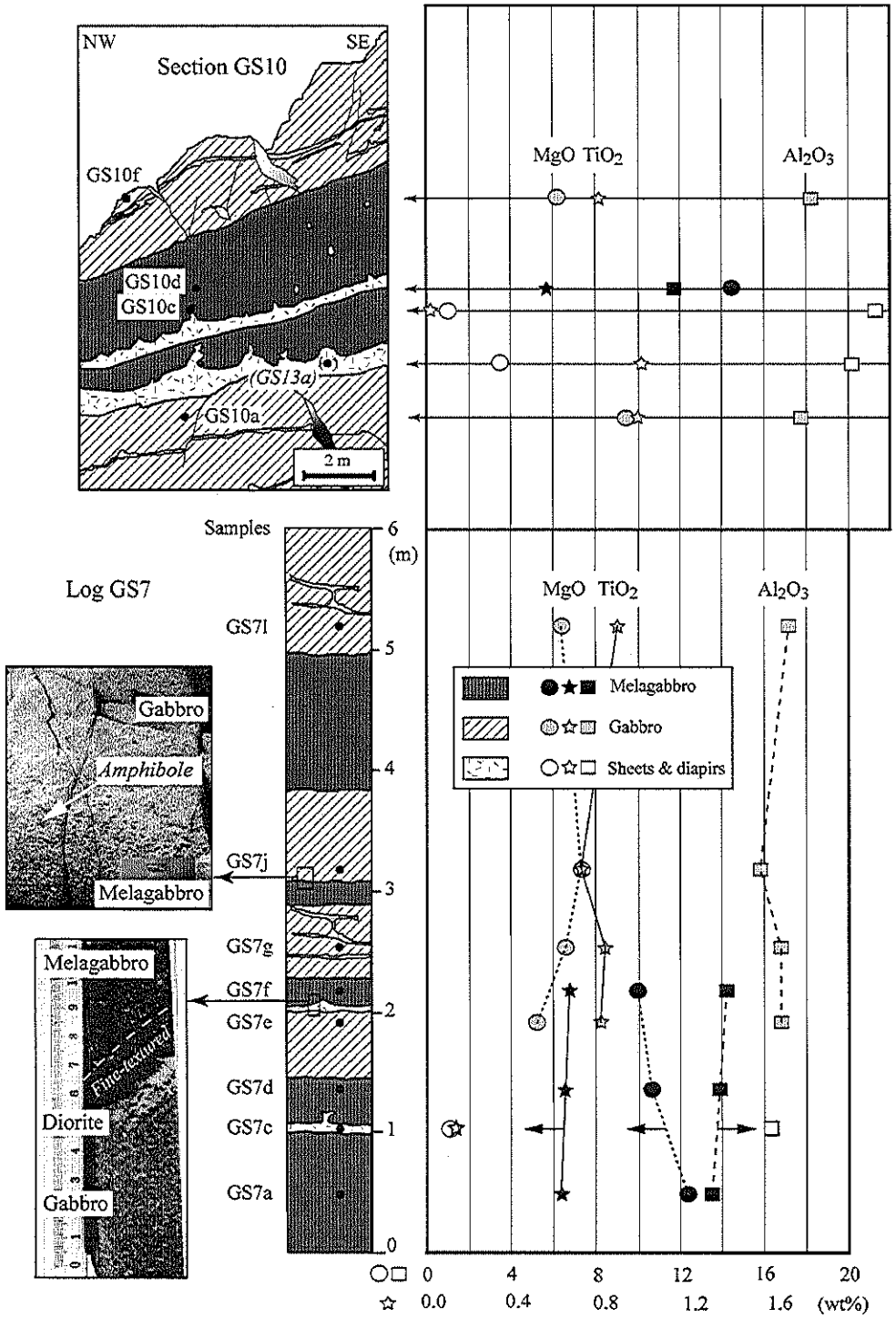
NW
SE
Section GS10
GS10f
GS10d
GS10c
(GS13a)
GS10a
2 m
Samples
Log GS7
GS7l
GS7j
GS7g
GS7f
GS7e
GS7d
GS7c
GS7a
6
(m)
5
4
3
2
1
0
Gabbro
Amphibole
Melagabbro
Melagabbro
Flinc-textured
Diorite
Gabbro
MgO TiO2
Al2O3
Melagabbro
Gabbro
Sheets & diapirs
0
4
8
12
16
20
0.0
0.4
0.8
1.2
1.6
(wt%)

Fig. 9

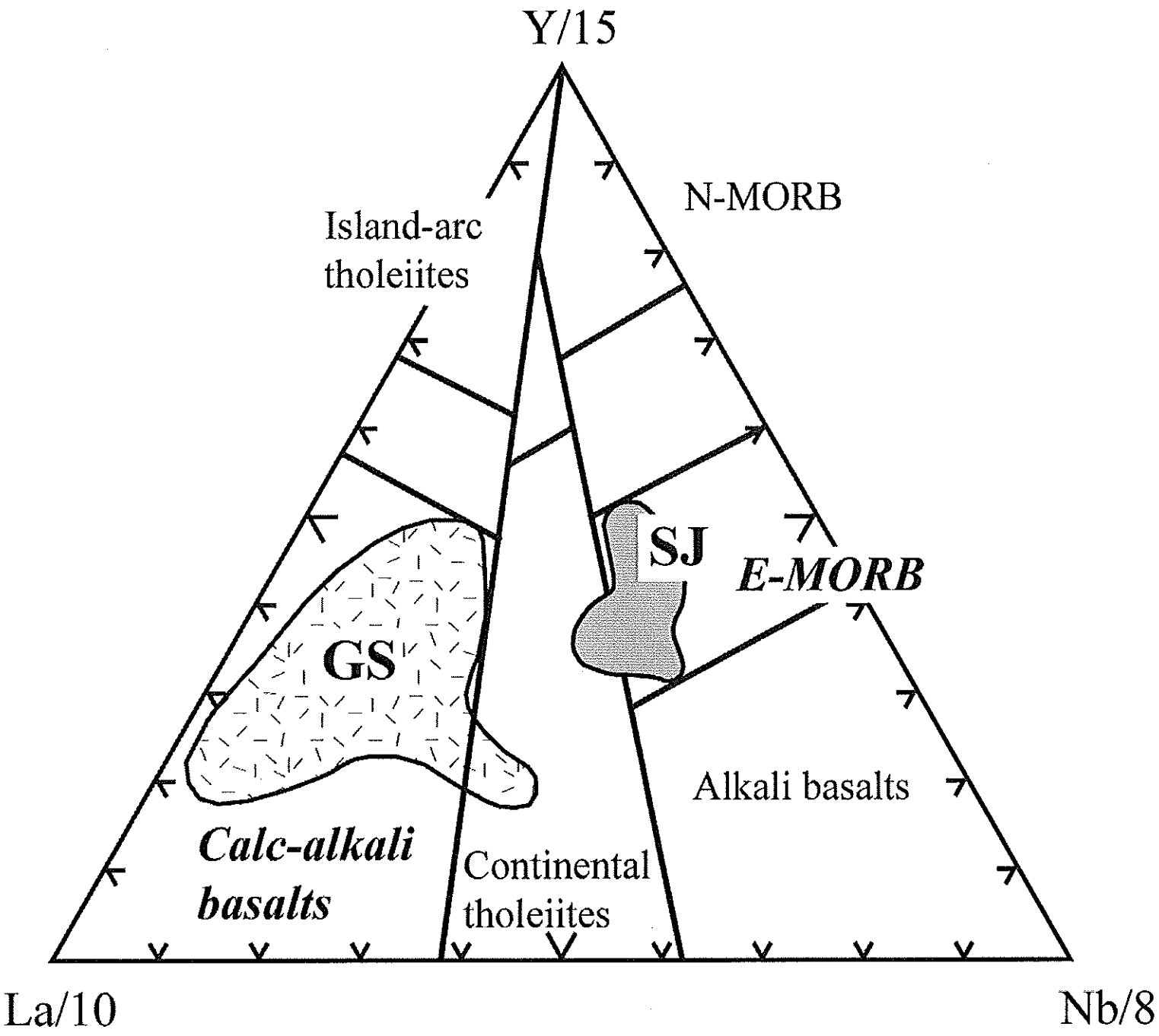
Y/15
N-MORB
Island-arc
tholeiites
SJ
E-MORB
GS
Alkali basalts
Calc-alkali
basalts
Continental
tholeiites
La/10
Nb/8

Fig. 10

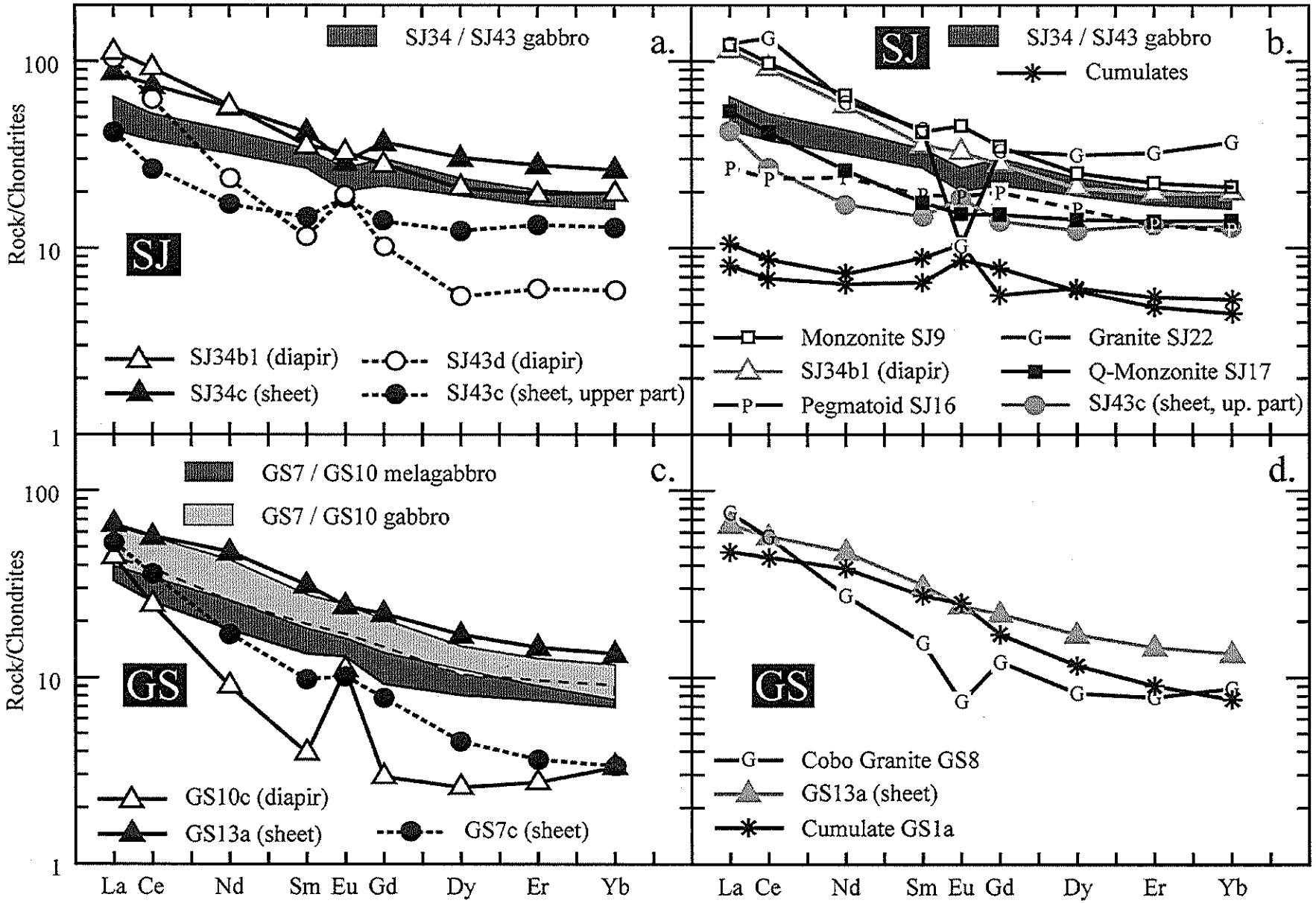
SJ34 / SJ43 gabbro
a.
SJ
Rock/Chondrites
100
10
1
SJ34b1 (diapir)
SJ43d (diapir)
SJ34c (sheet)
SJ43c (sheet, upper part)
b.
SJ
SJ34 / SJ43 gabbro
Cumulates
Monzonite SJ9
Granite SJ22
SJ34b1 (diapir)
Q-Monzonite SJ17
Pegmatoid SJ16
SJ43c (sheet, up. part)
c.
GS7 / GS10 melagabbro
GS7 / GS10 gabbro
GS
GS10c (diapir)
GS13a (sheet)
GS7c (sheet)
d.
GS
Cobo Granite GS8
GS13a (sheet)
Cumulate GS1a
La Ce Nd Sm Eu Gd Dy Er Yb

Fig. 11

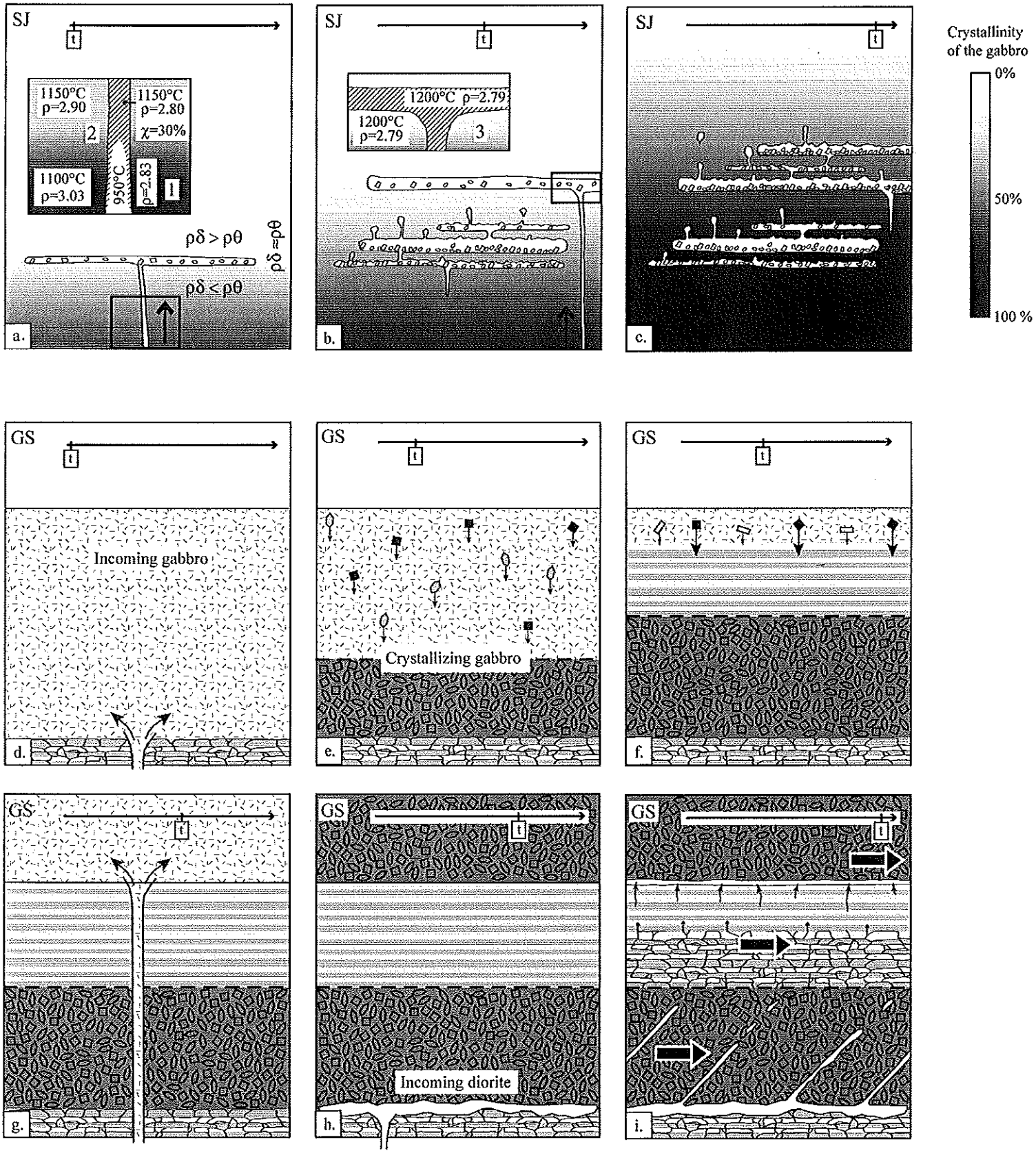
SJ
t
1150°C
ρ=2.90
1150°C
ρ=2.80
χ=30%
2
1100°C
ρ=3.03
950°C
ρ=2.83
1
ρδ > ρθ
ρδ ≈ ρθ
ρδ < ρθ
a.
1200°C ρ=2.79
1200°C
ρ=2.79
3
b.
c.
Crystallinity
of the gabbro
0%
50%
100 %
GS
Incoming gabbro
d.
Crystallizing gabbro
e.
f.
g.
Incoming diorite
h.
i.

Fig. 12

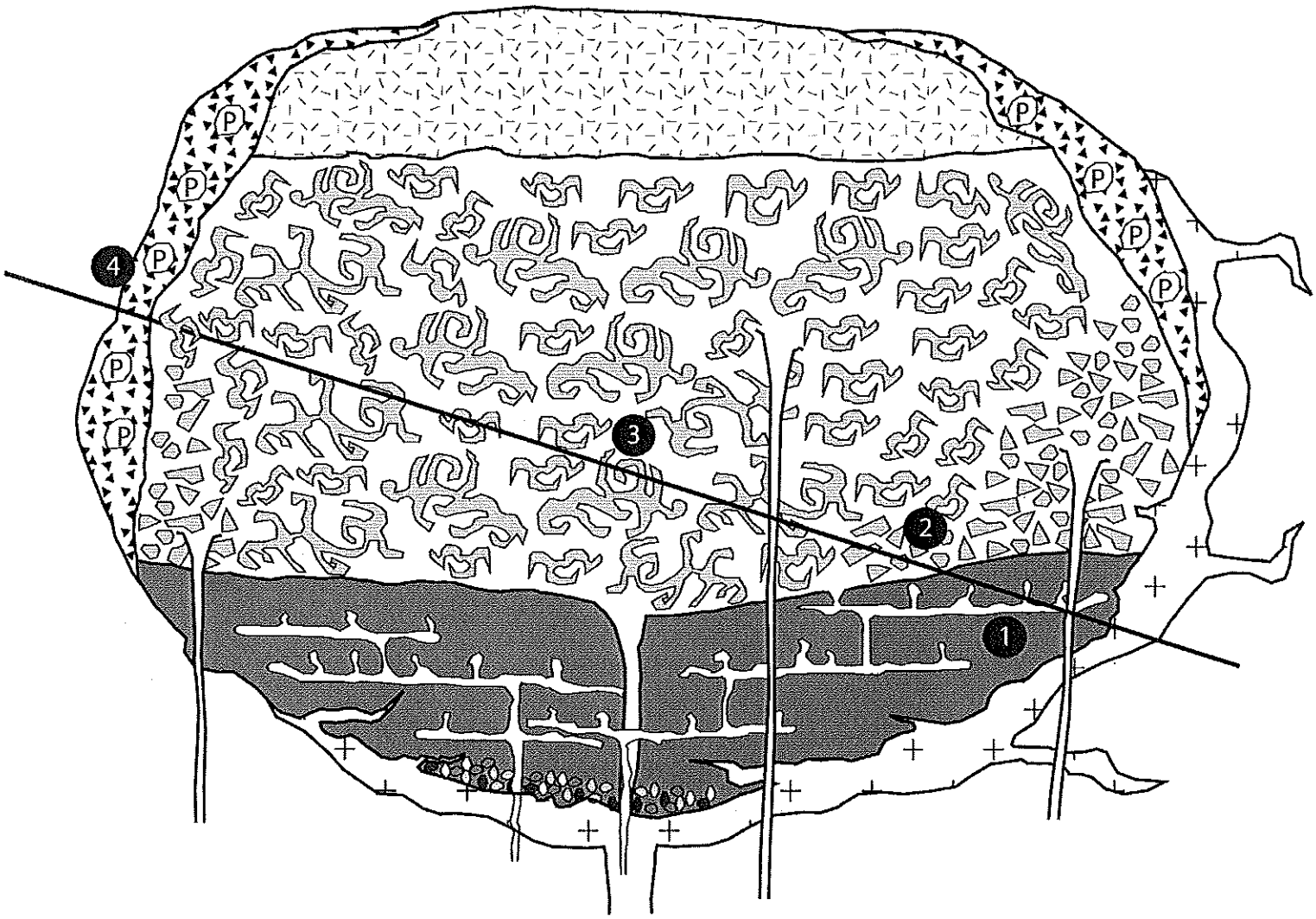

Granite

Hybridized magma

Lobate facies

Angular breccia

Plagioclase-rich cumulate

Pegmatoid

Diorite

Gabbro from Poul Rodou

Amphibole-rich cumulate

Cross-section from Poull Rodou (1) to Primel (4) through Saint-Jean (2, 3)

Fig. 13